Study of shape coexistence in Sn isotopes around A=110-120

EuNPC 2025

Giacomo Corbari
Università degli Studi di Milano and INFN

Shape coexistence in Sn isotopes

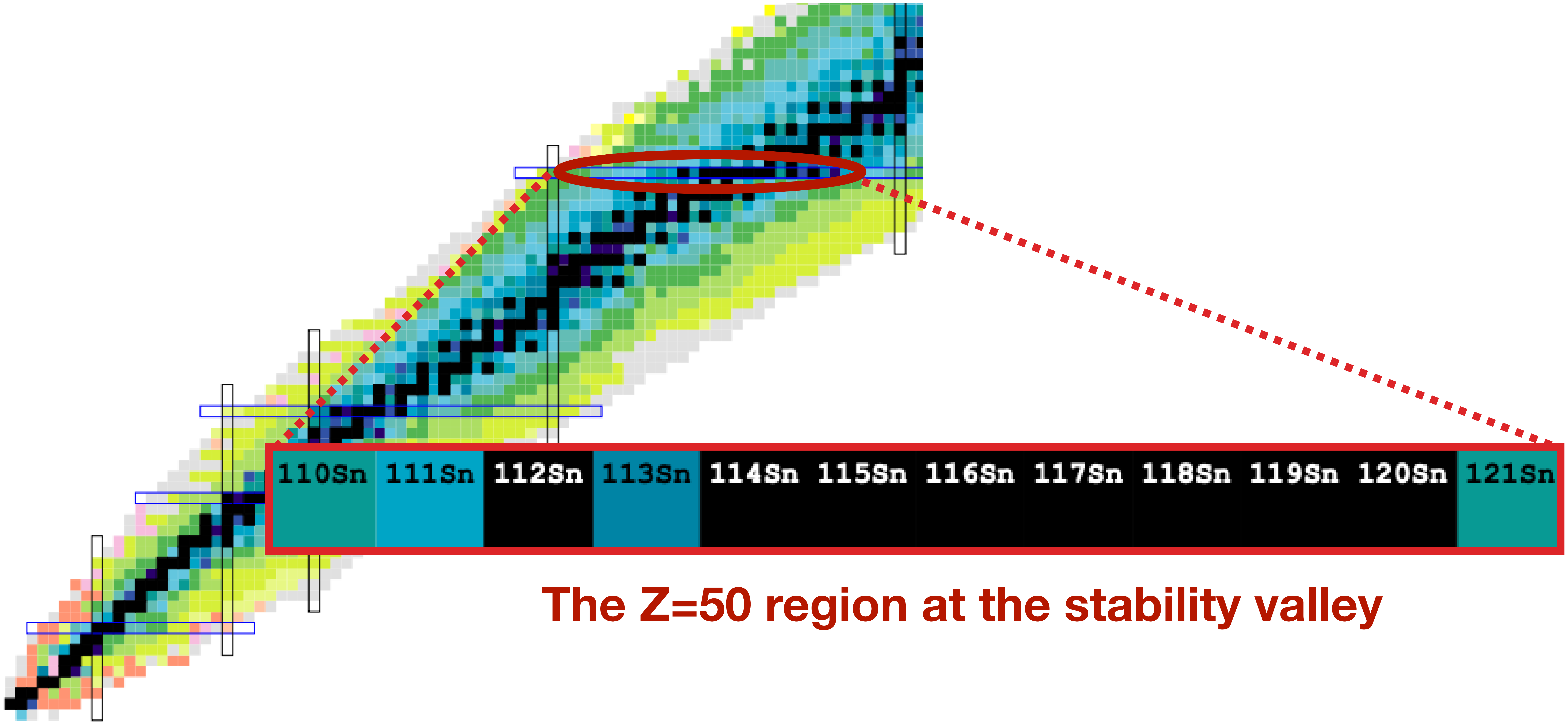

The Z=50 region at the stability valley

Shape coexistence in Sn isotopes

Level energies and bands

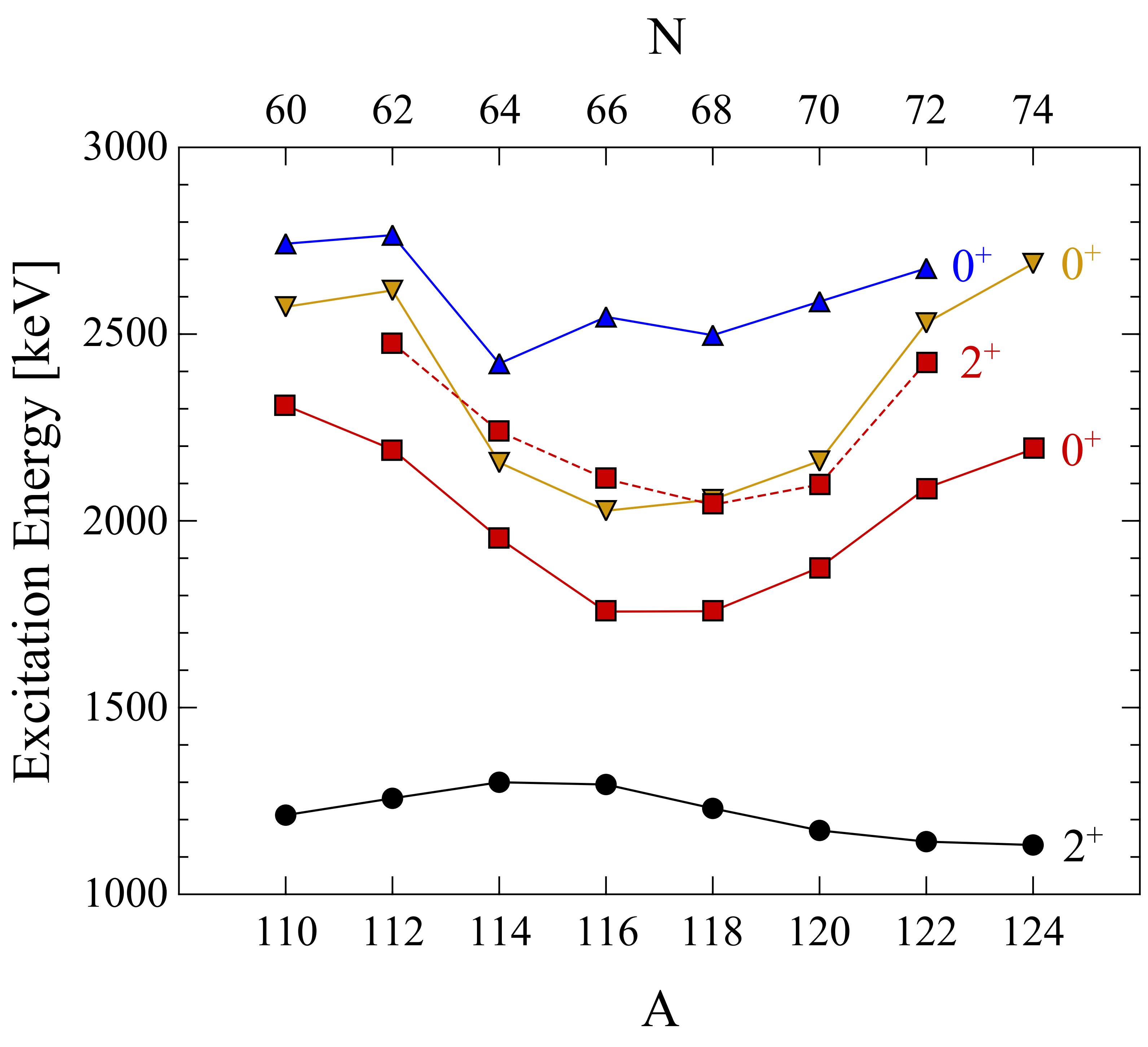

Intruder band built on 0_2^+

Transfer cross sections

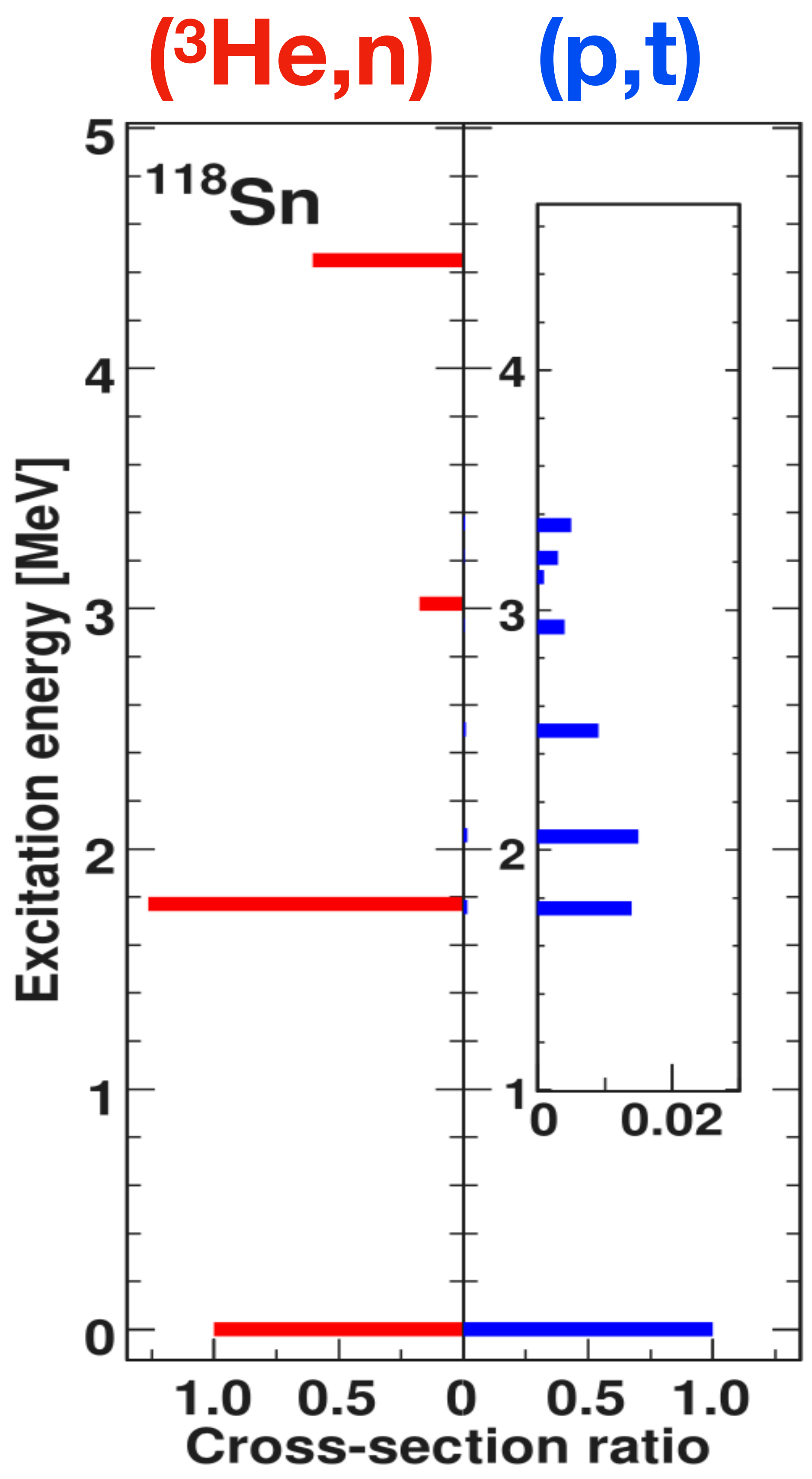

E2 and E0 transition probabilities

- $B(E2;0_2^+ \to 2_1^+) \gtrsim 10$ W.u.
- Large $\rho^2(E0;0_3^+ \to 0_2^+)$: strong mixing or large $\Delta\beta$

A complex scenario!

Shape coexistence in Sn isotopes

Excitations across Z=50 shell gap

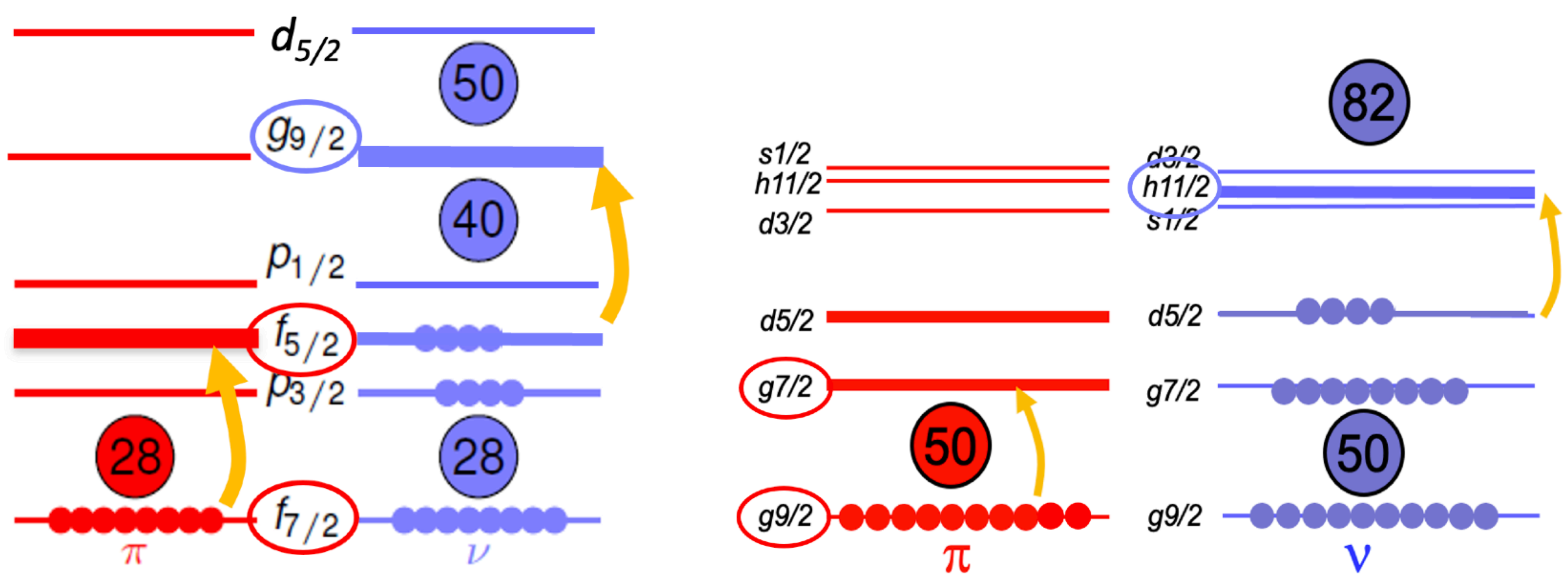

^{64}Ni ^{112}Sn

Expected similar scenario to Ni

Spontaneus simmetry breaking

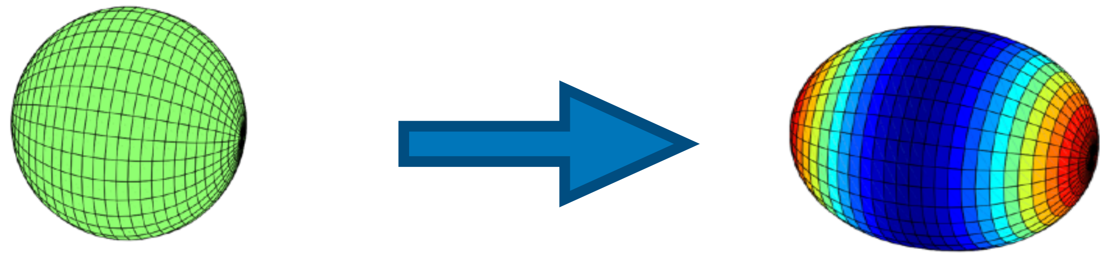

Induced by proton-neutron interaction

Monte Carlo Shell Model PES

T. Togashi et al., Phys. Rev. Lett. 121, 062501 (2018).

T. Otsuka, Y. Tsunoda, to be published.

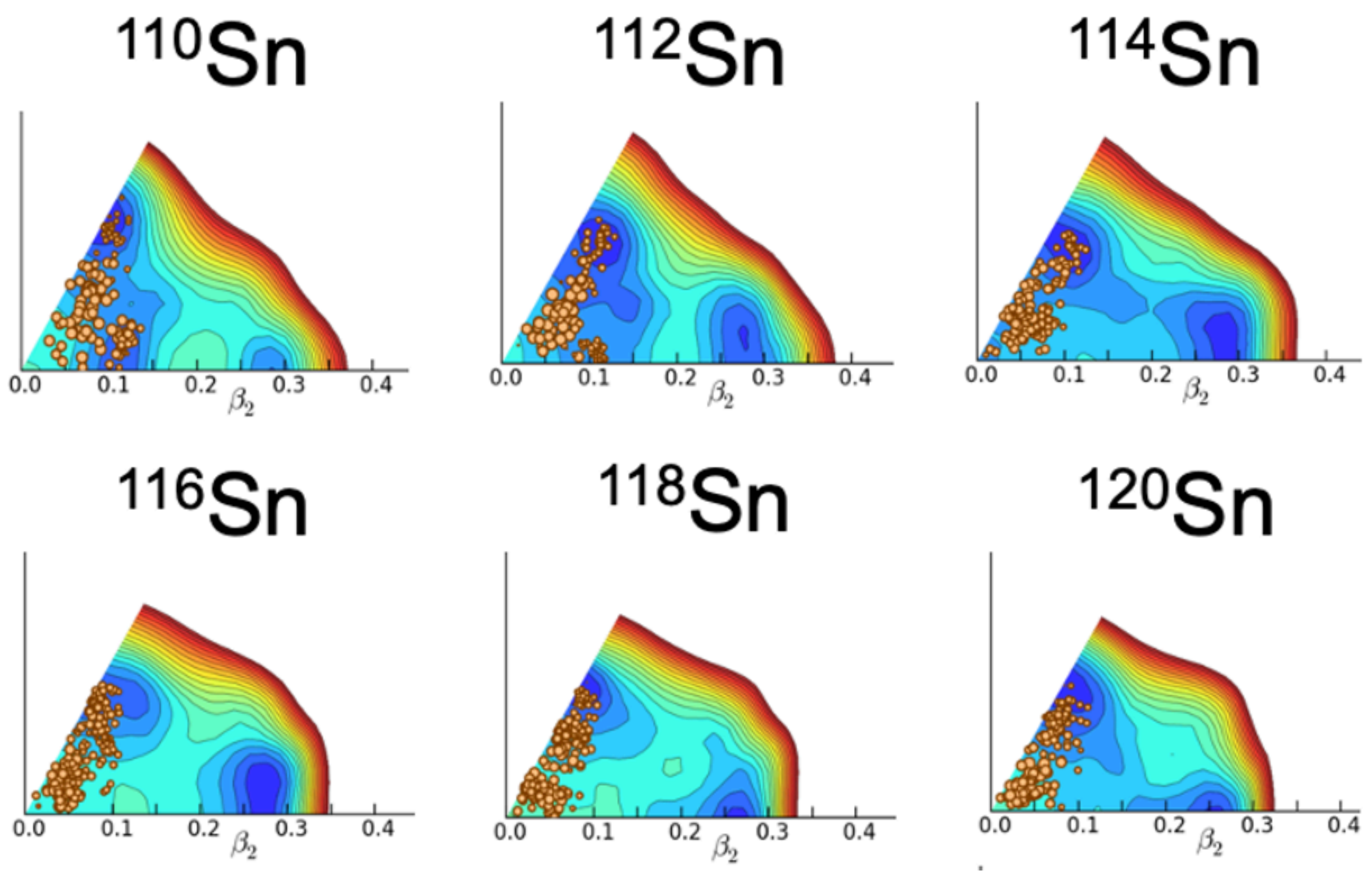

Well-separated prolate minimum appearing from ^{112}Sn up to ^{118}Sn

How to probe shape coexistence?

Lifetime measurements of 0^+ states! → Many 0^+ states observed → Many unknown lifetimes!

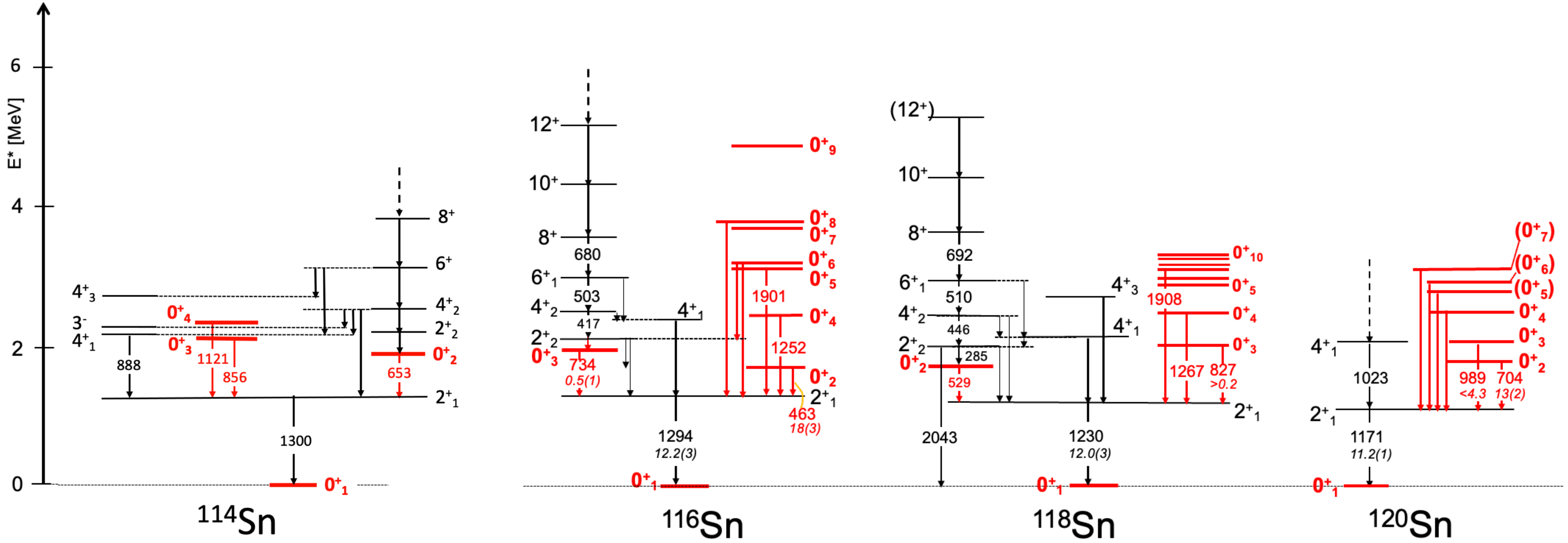

Experiments @ IFIN-HH

Heavy-ion transfer reactions near the Coulomb barrier

$^{18}O + ^{112}Sn$ @ 59 MeV
$^{13}C+^{117}Sn$ @ 43 MeV
$^{13}C+^{119}Sn$ @ 43 MeV
$^{16}O+^{116}Cd$ @ 56 MeV

ROSPHERE

- 25 HPGe+BGO

SORCERER

- 6 Si solar cells

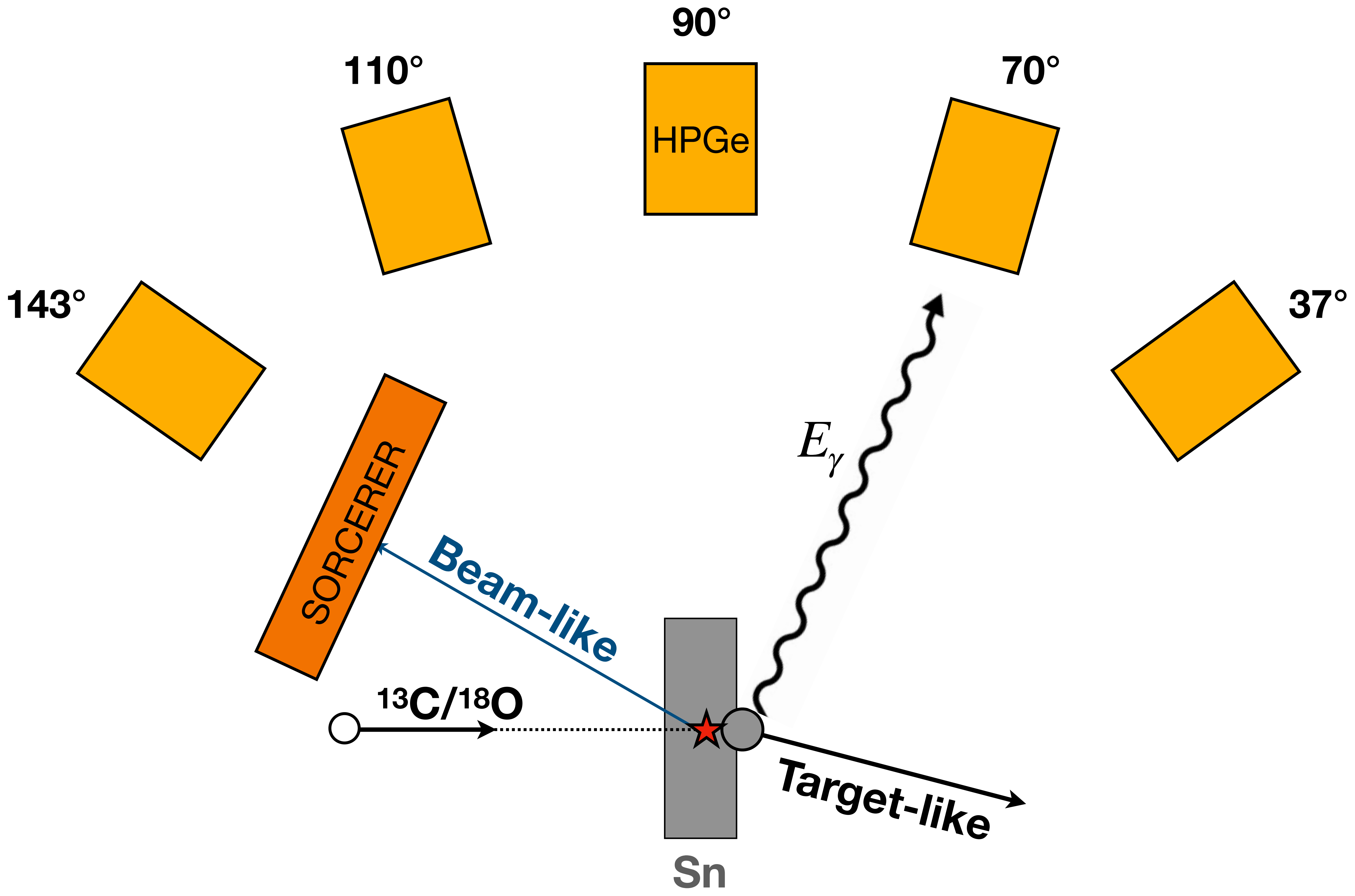

D. Bucurescu et al., NIM A 837 (2016) 1–10
T. Beck et al., NIM A 951 (2020) 163090

Spectroscopy with thick targets

- n, p, α transfer reactions

  $^{114}Sn \Longrightarrow$ -2n

  $^{116}Sn \Longrightarrow$ +1n

  $^{118}Sn \Longrightarrow$ +1n, -1n, -2p

  $^{120}Sn \Longrightarrow$ -1n, -1α

- Cd and Sn targets (~10 mg/cm^2)
- ^{13}C and $^{16,18}O$ beams @ Coulomb barrier energies

Level schemes, relative population yields of 0^+ states

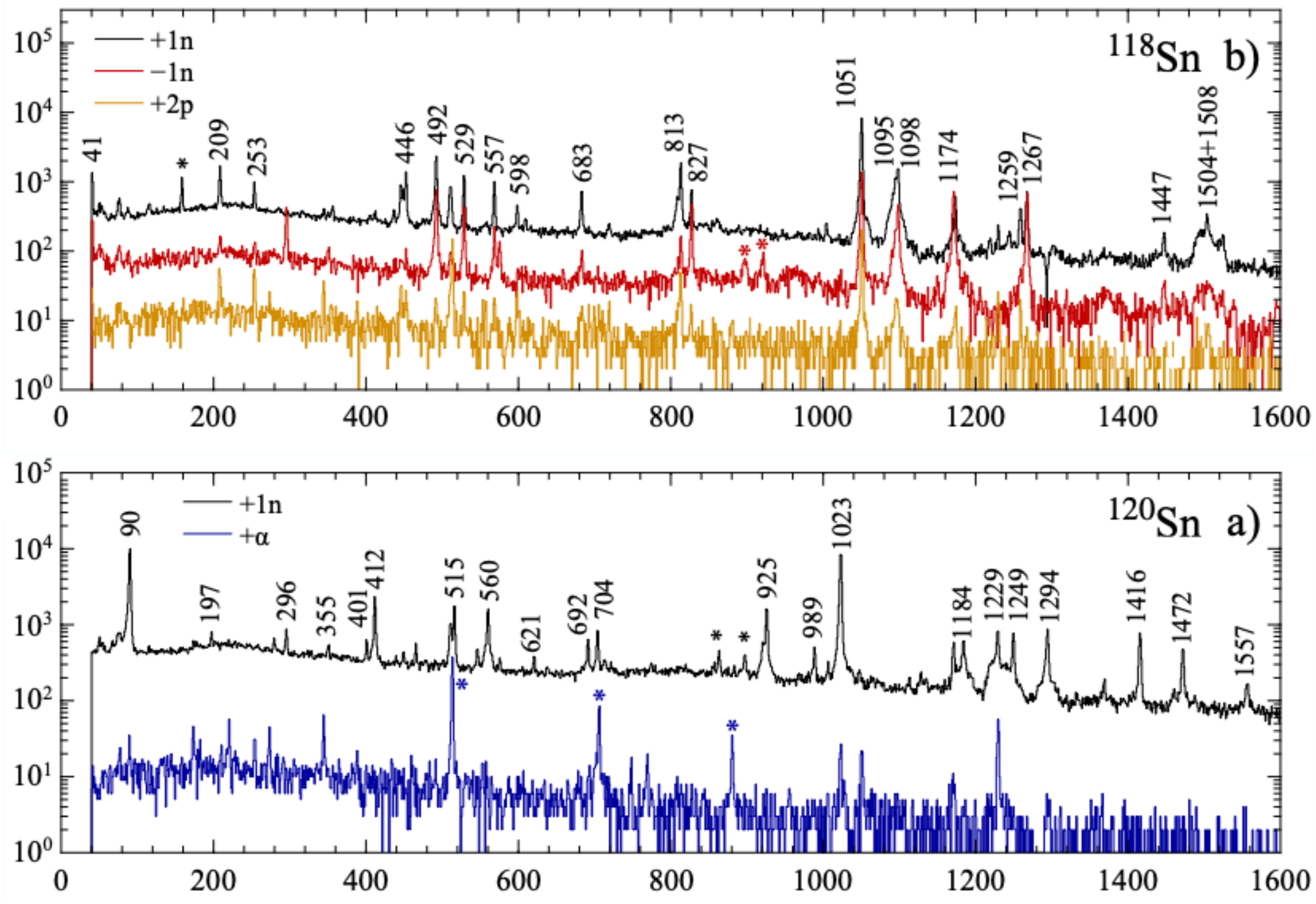

Population of 0^+ states

- n, p, α transfer reactions

  $^{114}Sn \Longrightarrow$ -2n

  $^{116}Sn \Longrightarrow$ +1n

  $^{118}Sn \Longrightarrow$ +1n, -1n, -2p

  $^{120}Sn \Longrightarrow$ -1n, -1α

- Cd and Sn targets (~10 mg/cm^2)
- ^{13}C and $^{16,18}O$ beams @ Coulomb barrier energies

Level schemes, relative population yields of 0^+ states

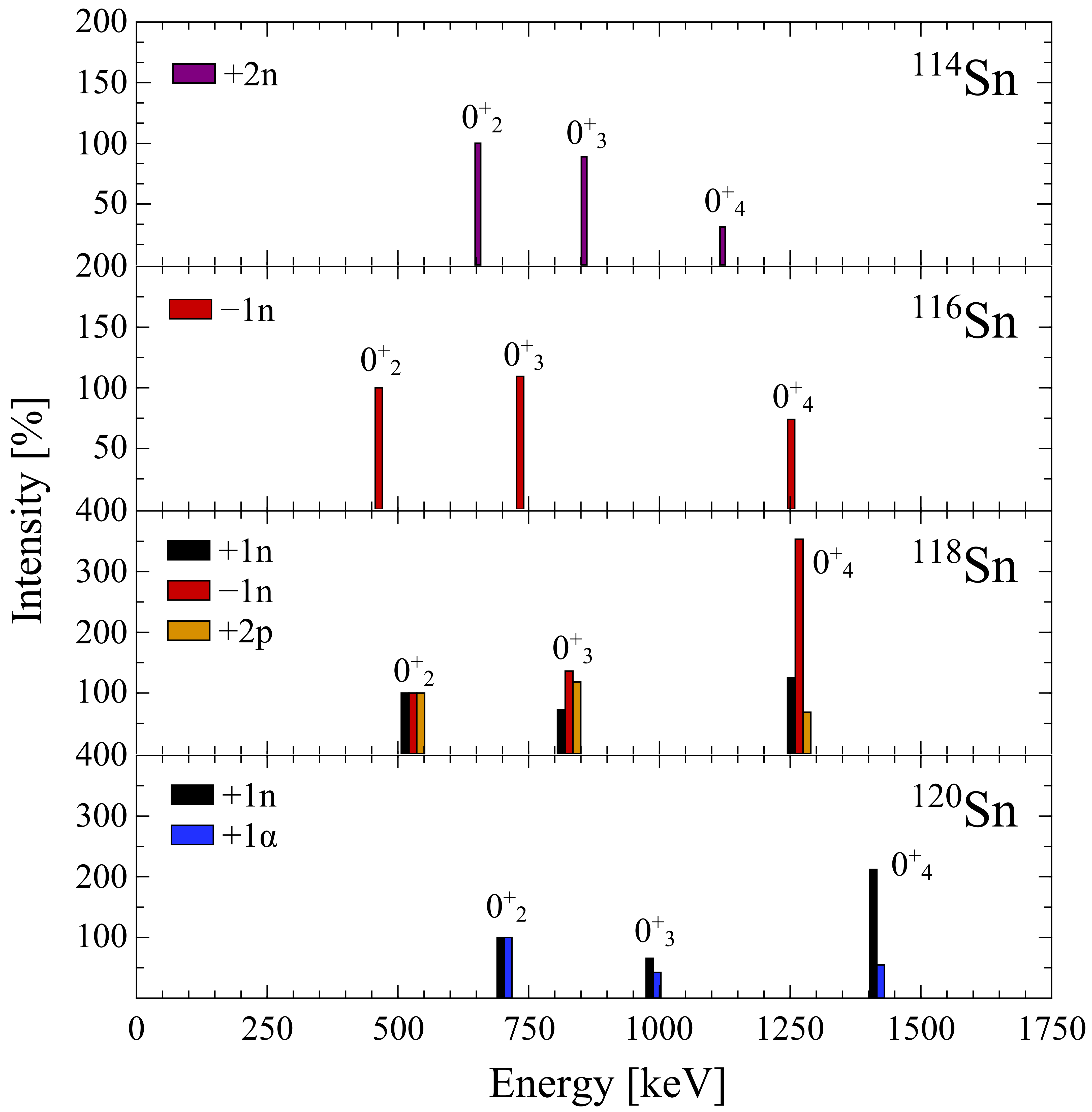

Lifetimes with Doppler-shift methods

Doppler Shift Attenuation

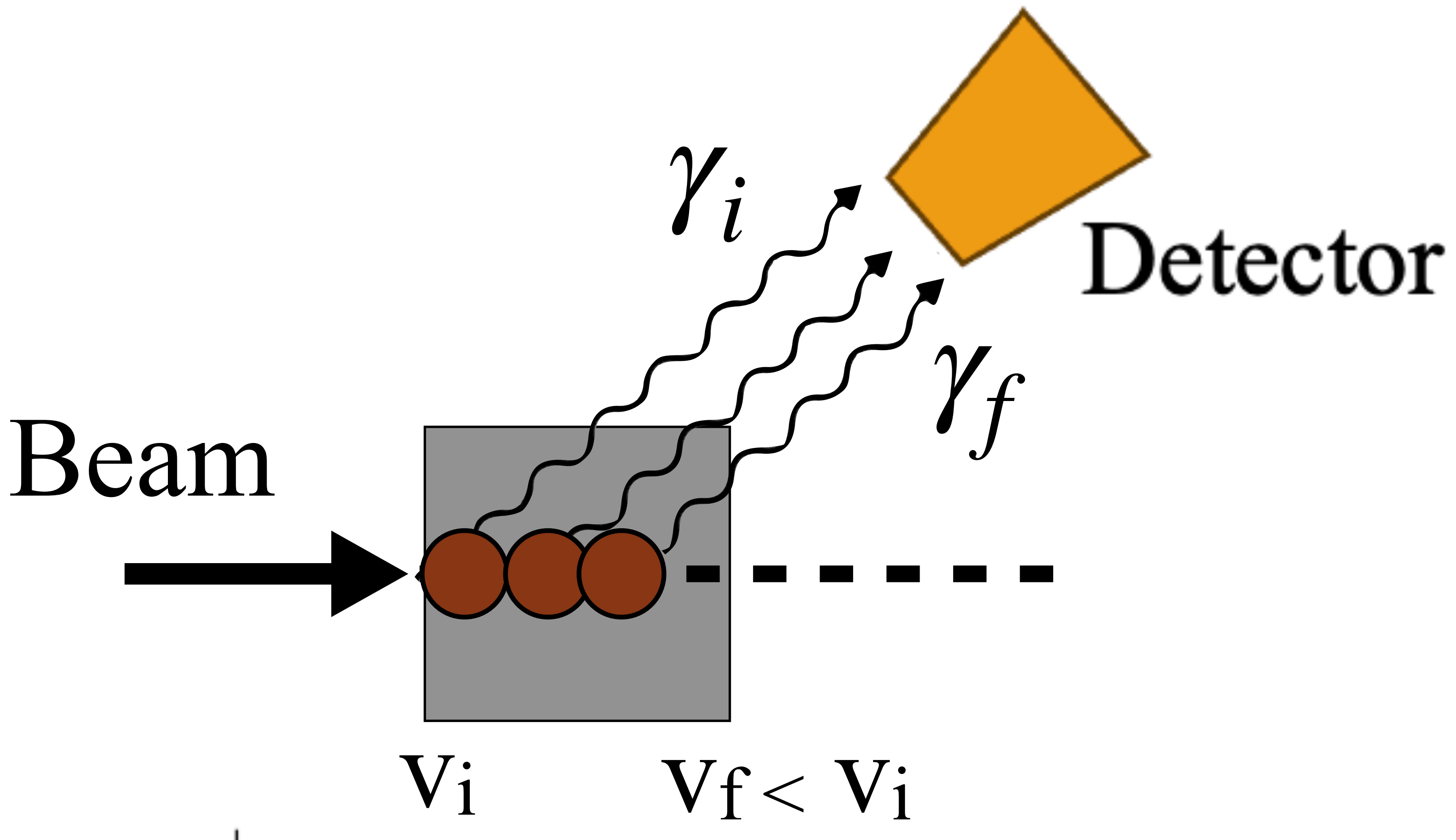

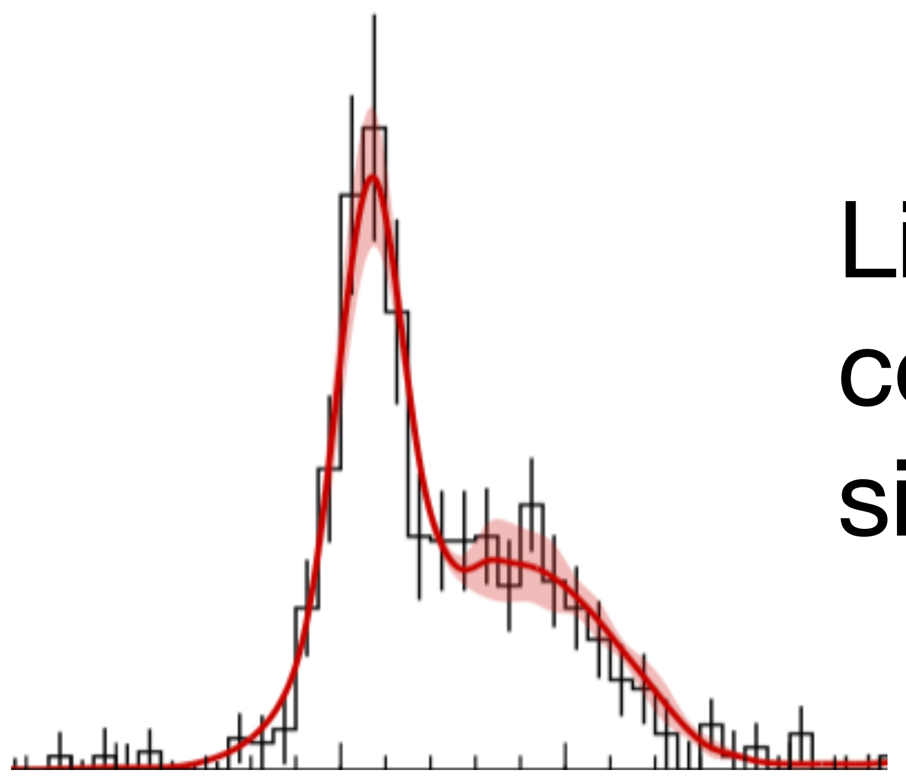

Lifetimes from comparison with simulated **lineshape**

Recoil Distance Doppler Shift

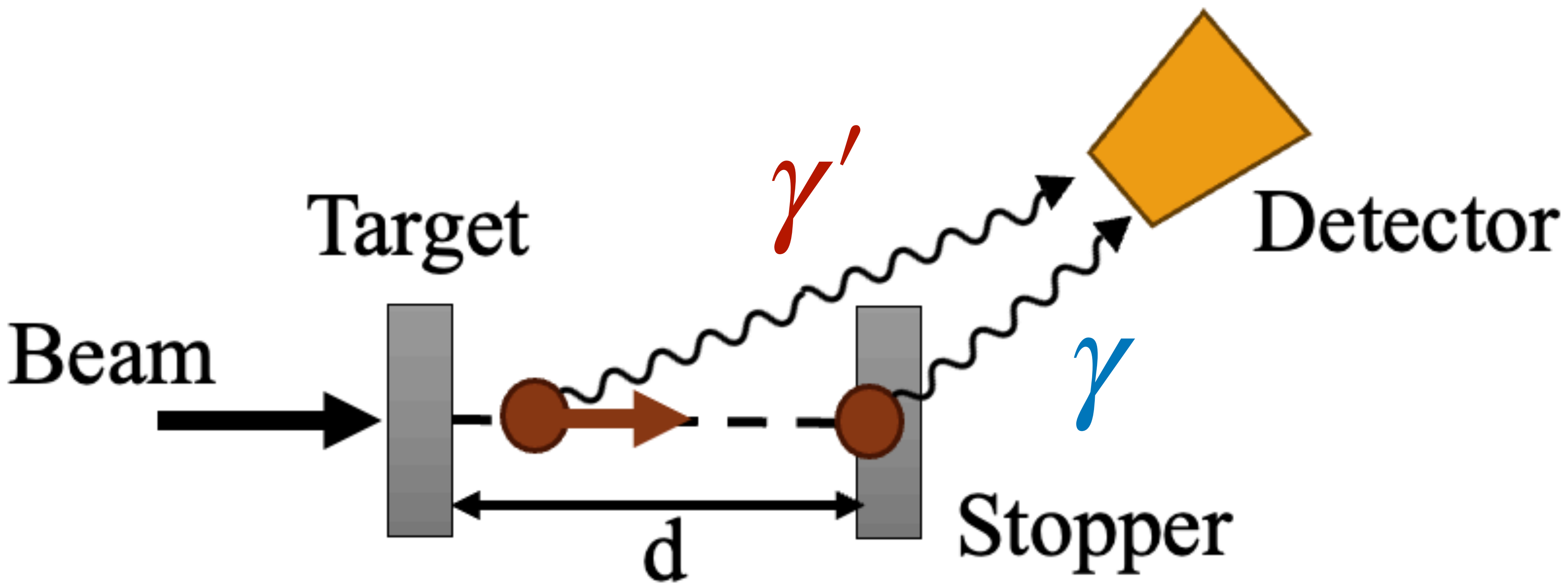

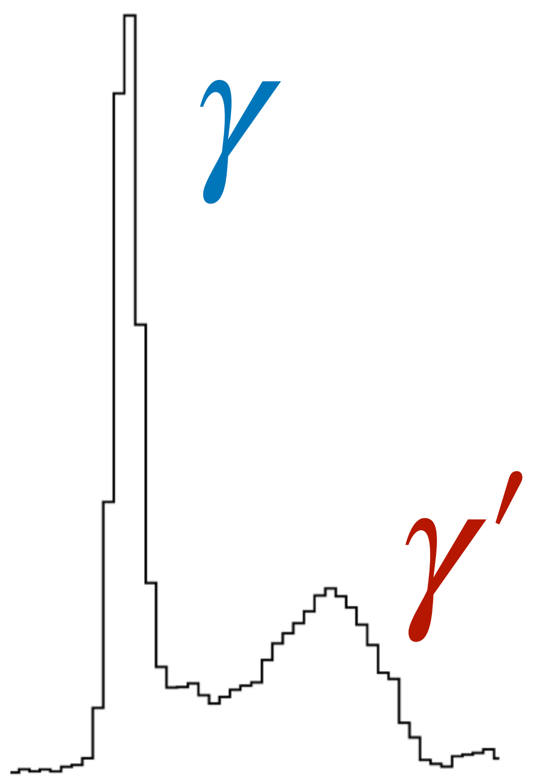

Lifetimes from the ratio of **stopped** and the **shifted** components

DSAM implementation for ROSPHERE

Methods

Newly developed Monte Carlo simulations for Doppler Shift Attenuation Method

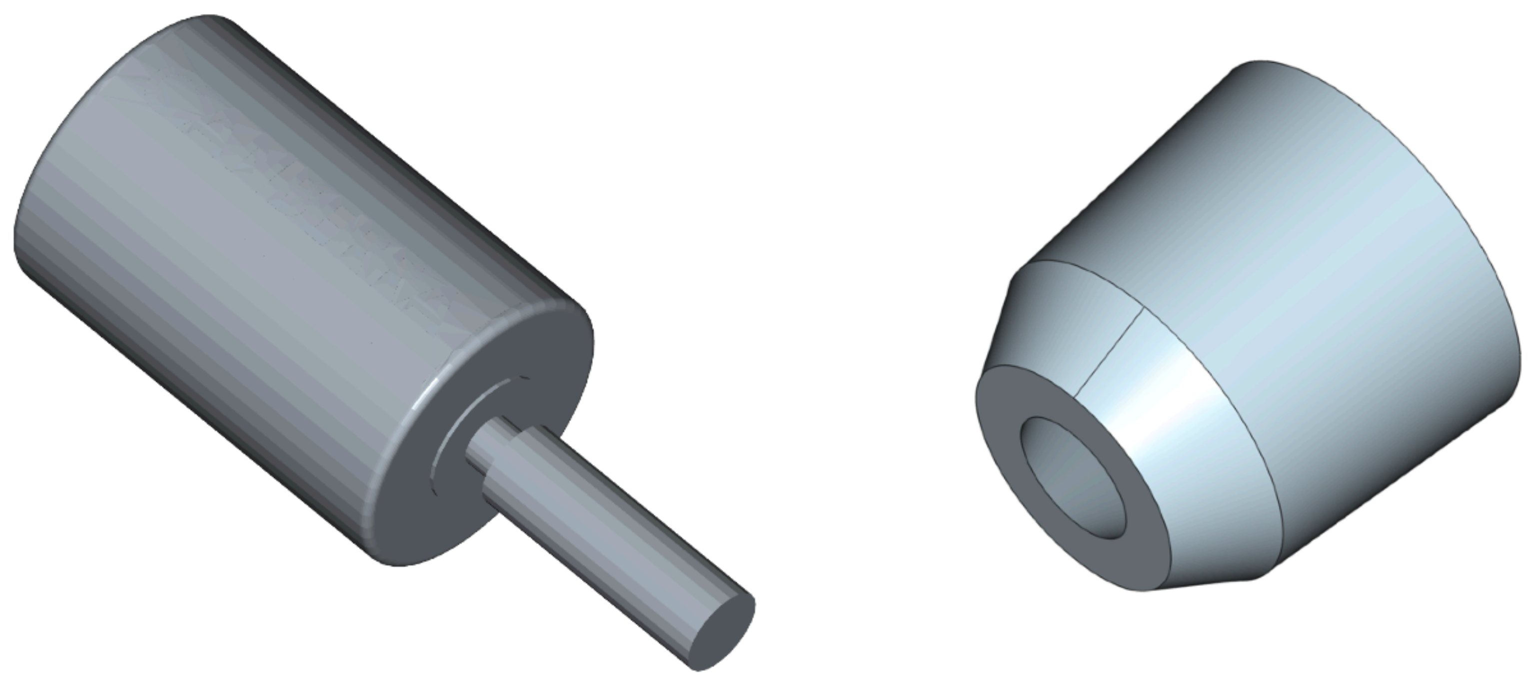

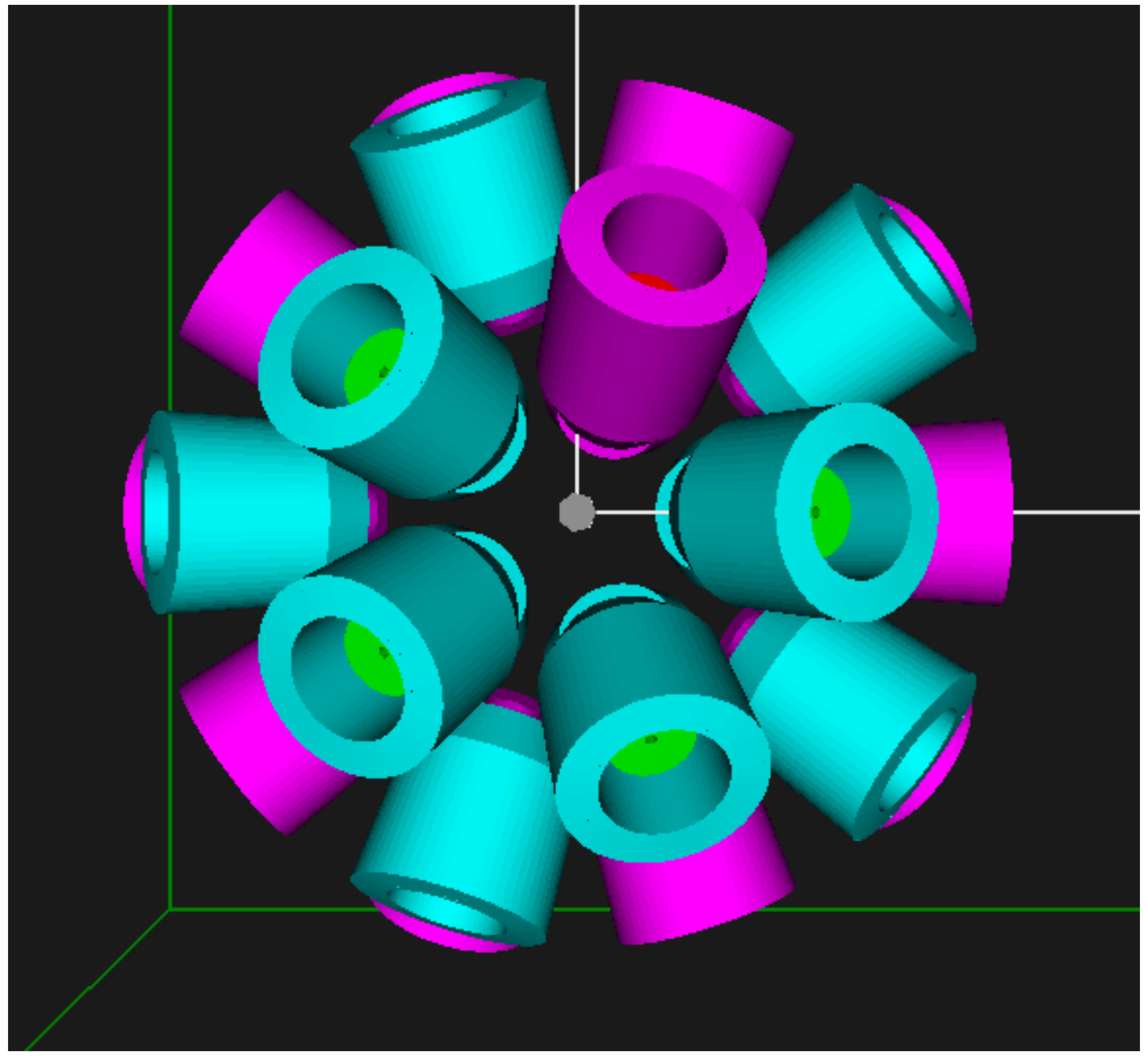

→ Implemented within the AGATA simulation code framework (GEANT4)

→ Use of CAD drawings of ROSPHERE detectors (HPGe + BGO shields)

DSAM benchmarks

DSAM on thick targets datasets

- ±1n transfer reactions
- ^{117,119}Sn targets
- ^{13}C beam around barrier energies

Good agreement with data available in literature!

State	Literature	This work
1^+_1	640 ±12 fs	644^{+60}_{-53} fs
2^+_1	130^{+60}_{-30} fs	174^{+14}_{-13} fs

^{120}Sn : $1^+_1 \rightarrow 2^+_1$ 1664 keV

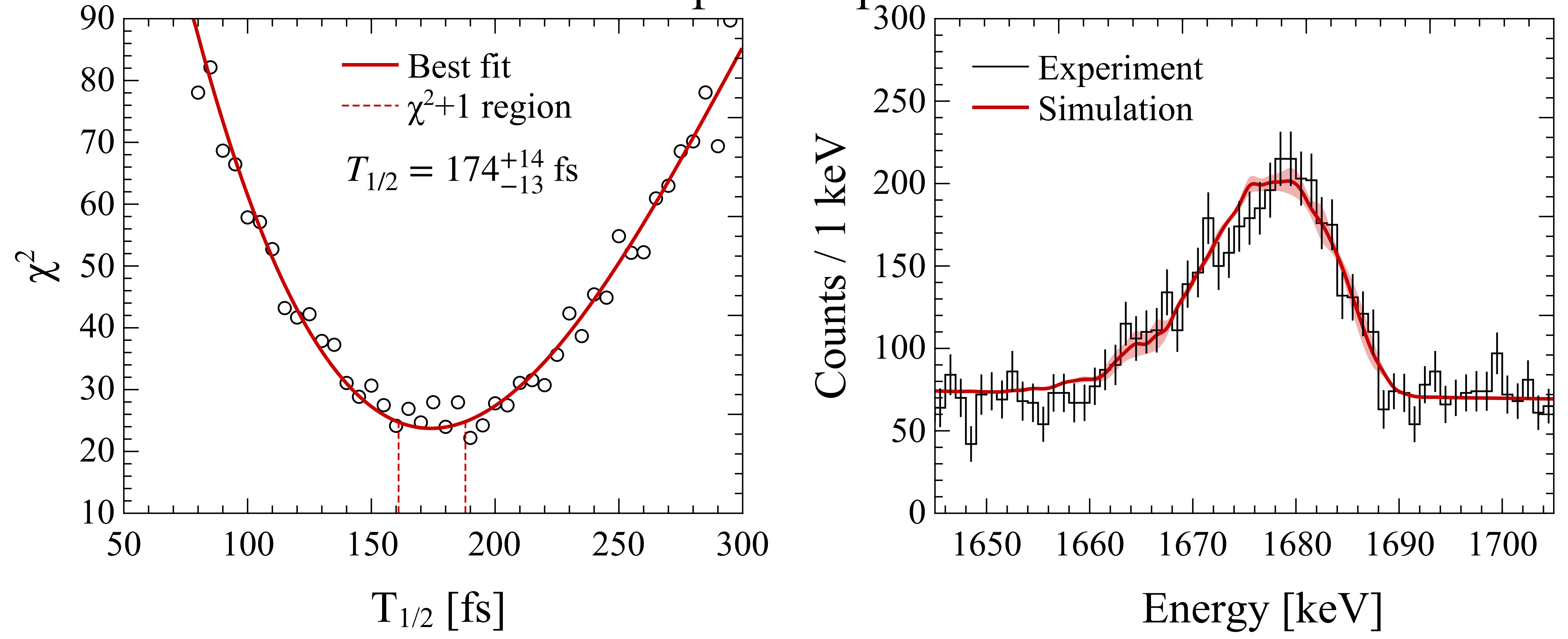

^{120}Sn : $2^+_1 \rightarrow 0^+_1$ 1171 keV

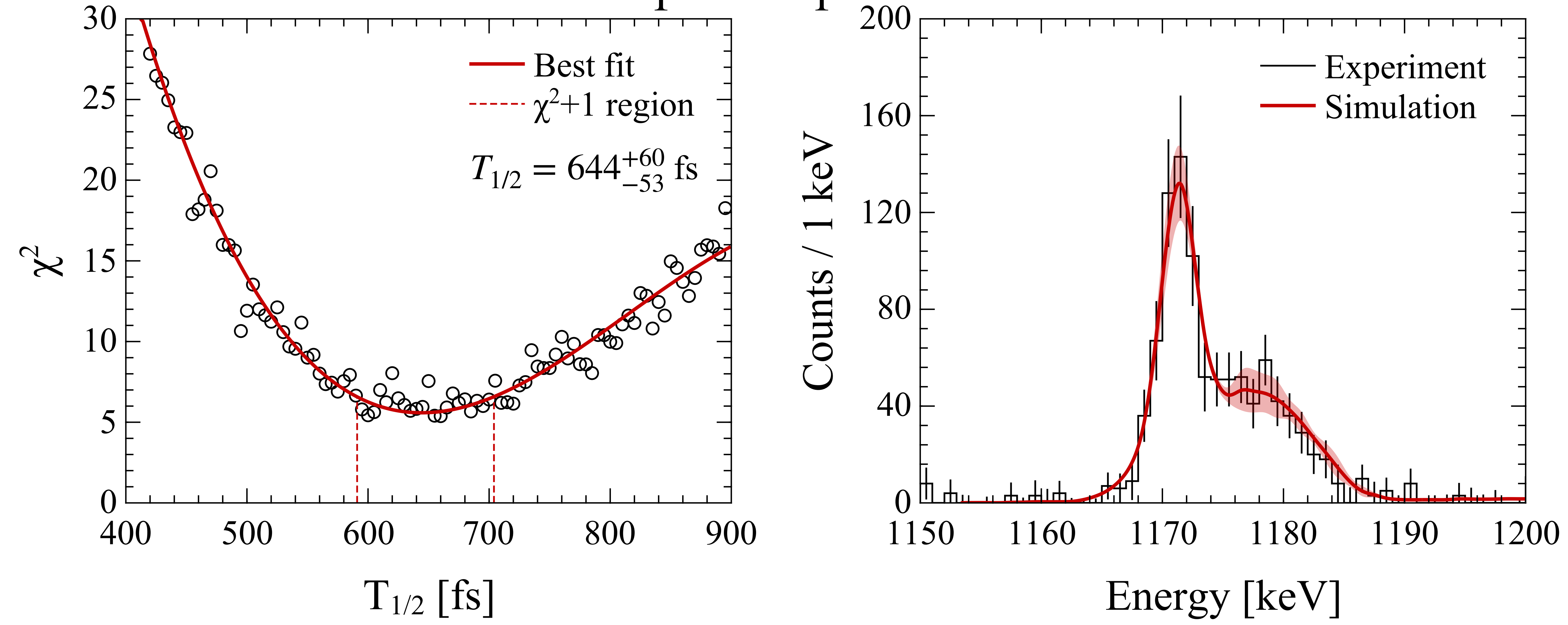

Lifetime of the 0^+_4 state of ^{116}Sn

$$^{116}\text{Sn} : 0^+_4 \rightarrow 2^+_1 \ 1252 \text{ keV}$$

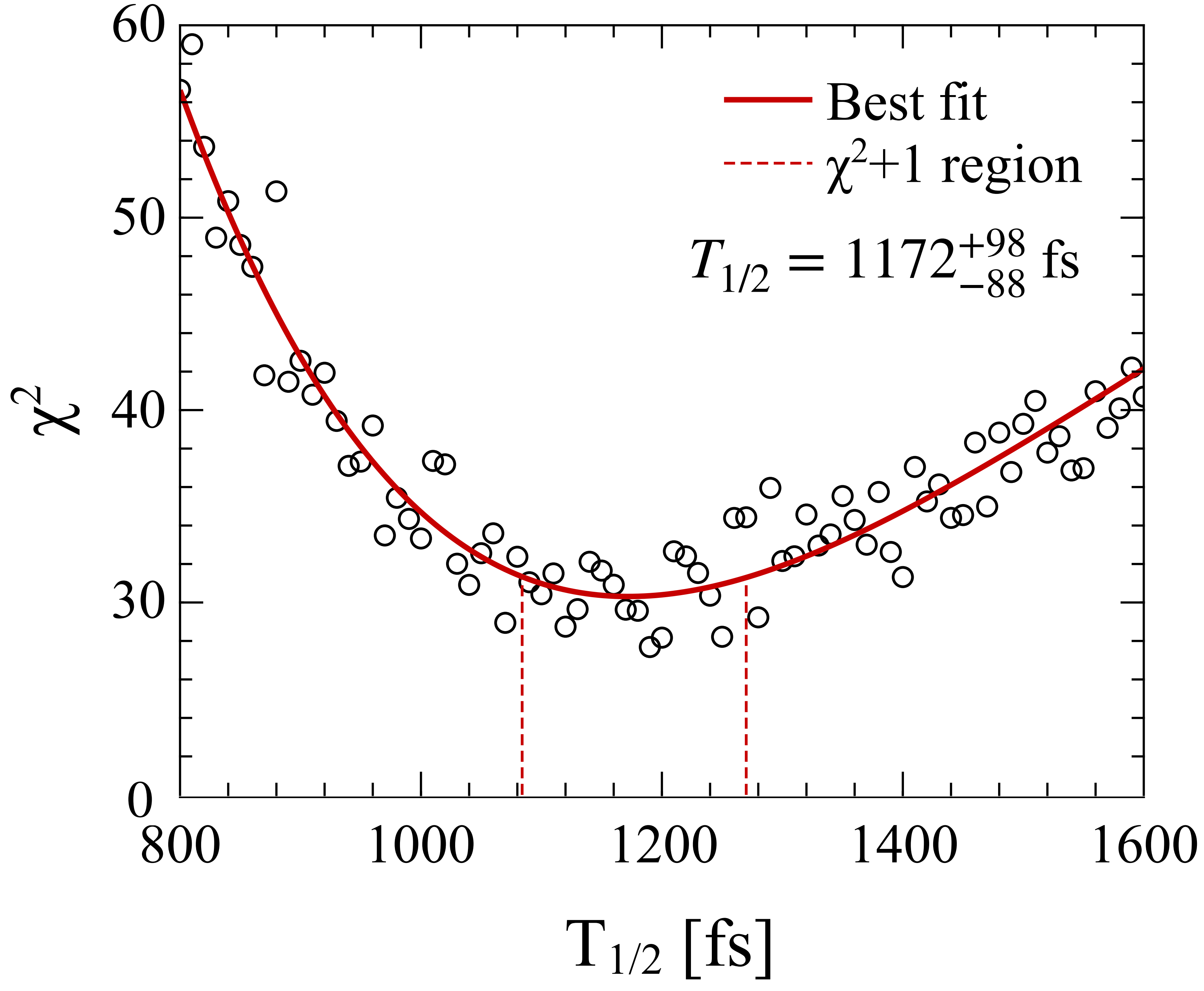

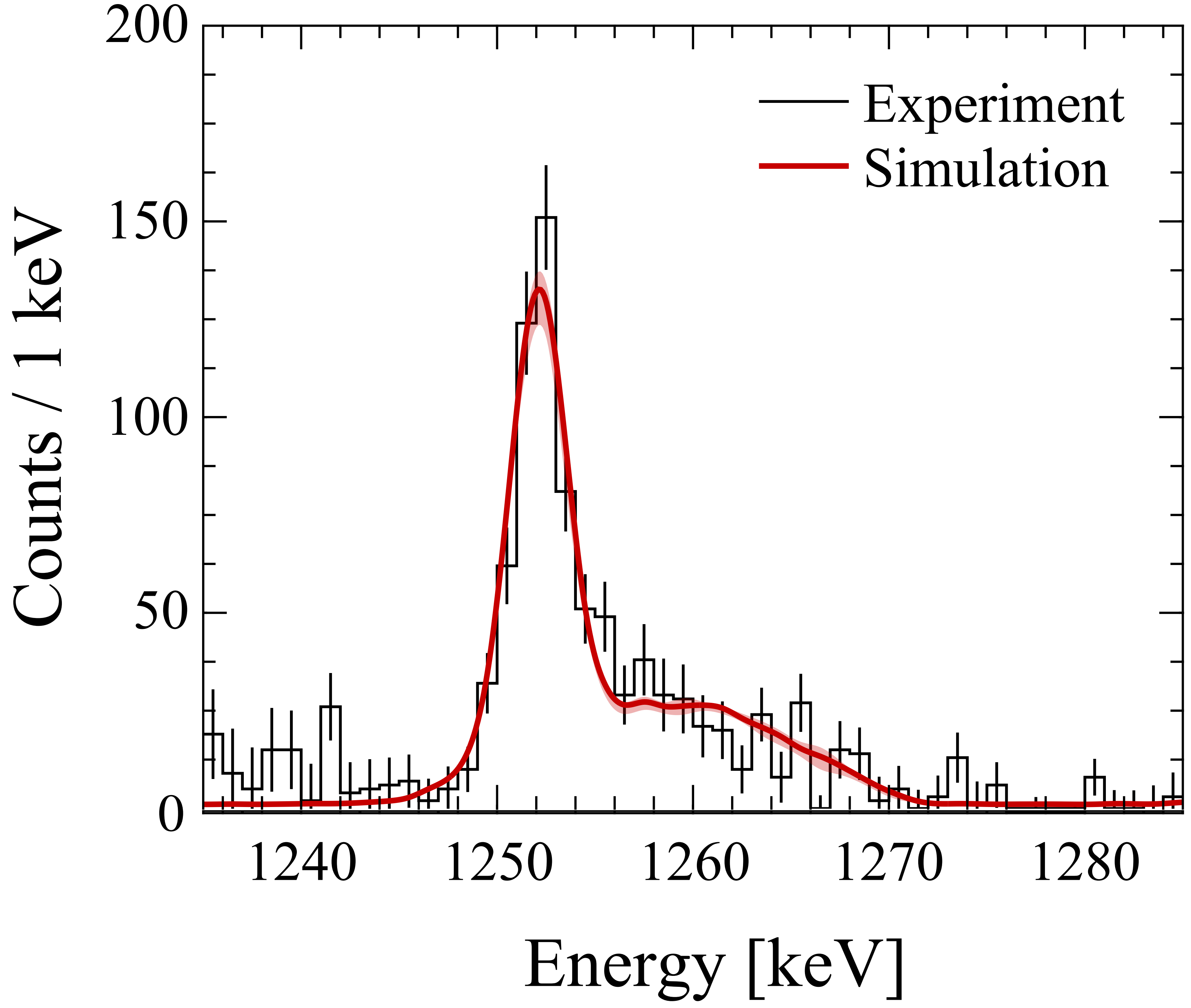

$$T_{1/2} = 1172^{+98}_{-88} \text{ ps}$$

RDDS experiments

$^{112}Sn(^{18}O,^{16}O)^{114}Sn$ @ 59 MeV

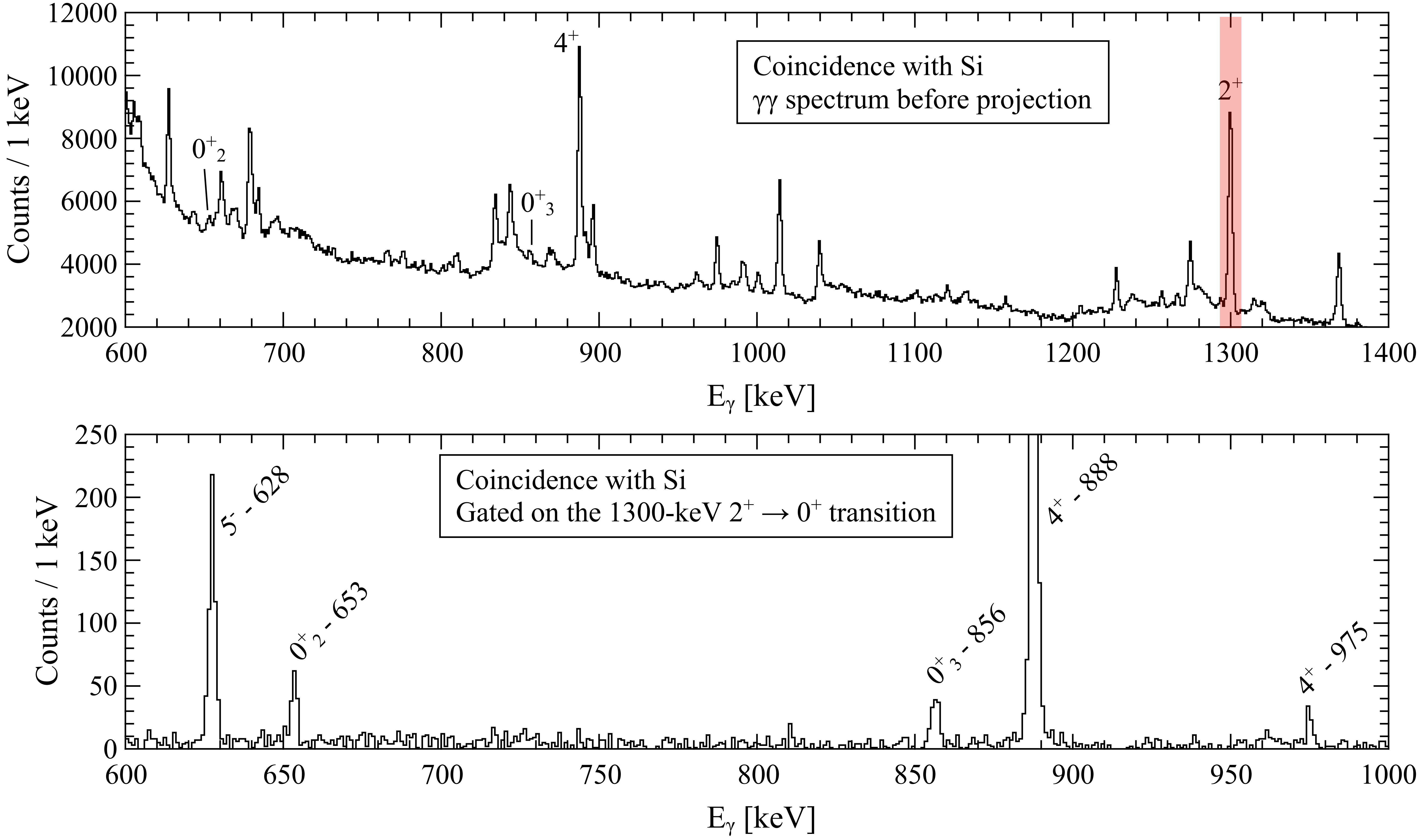

RDDS technique

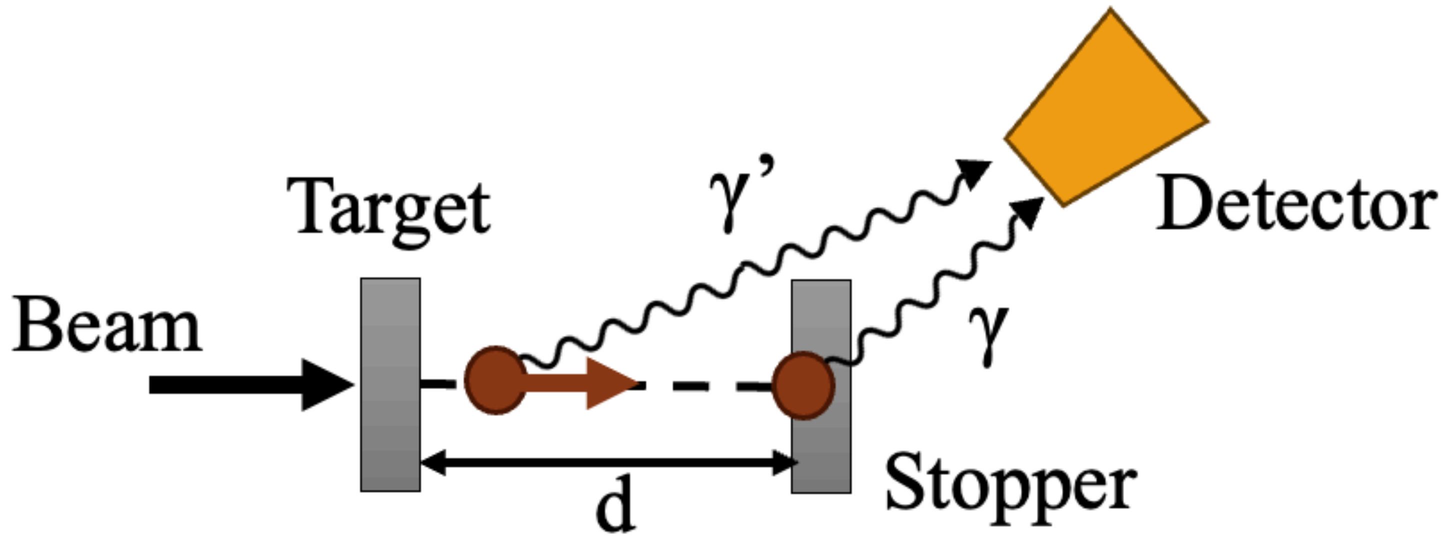

$\gamma\gamma$ coincidence method

No significant feeding observed or expected from higher lying states

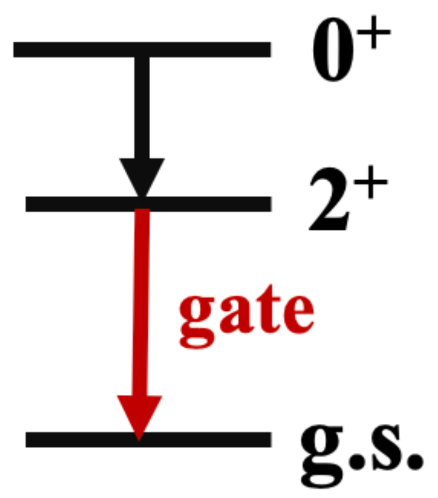

The ^{118}Sn case

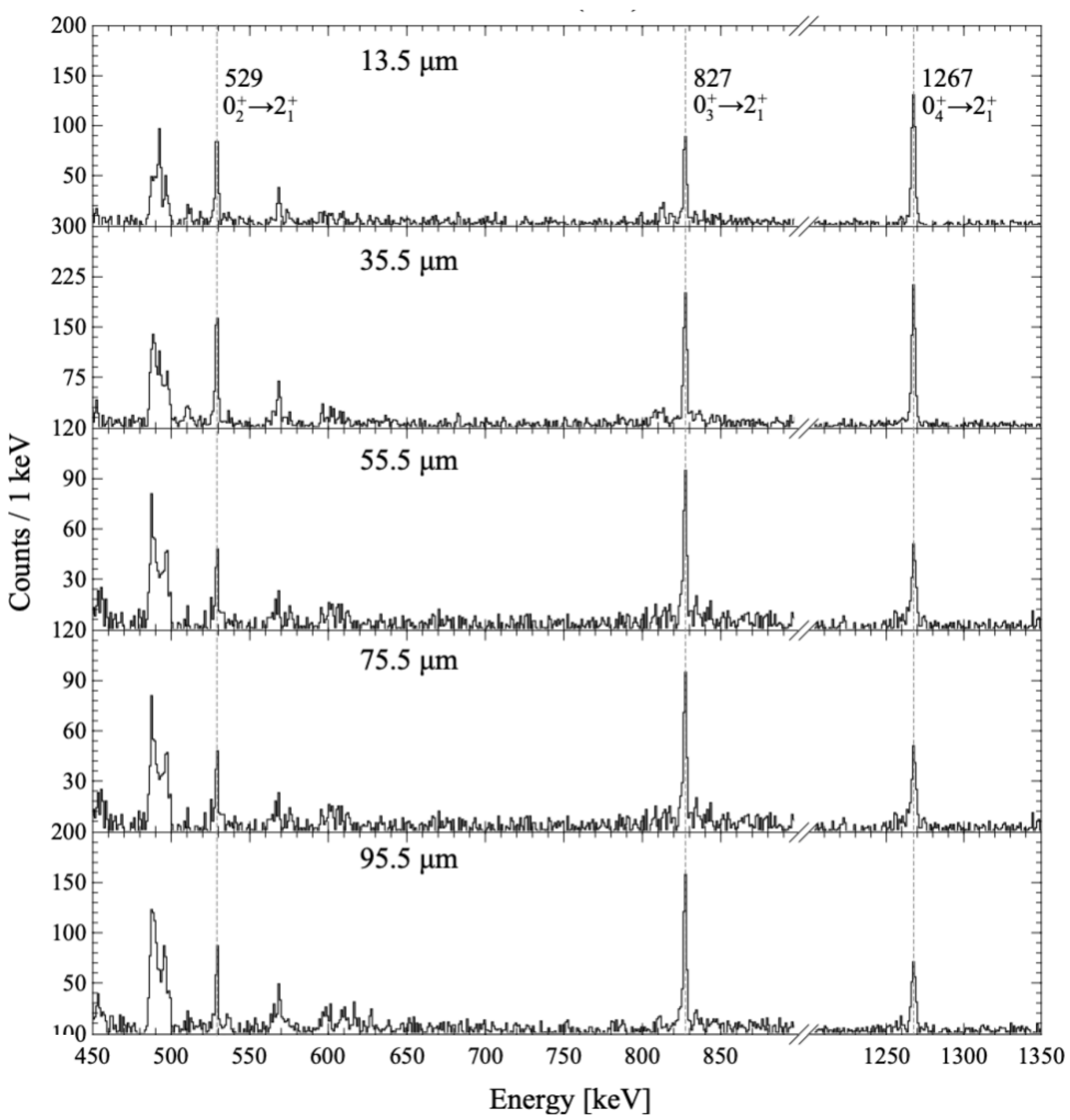

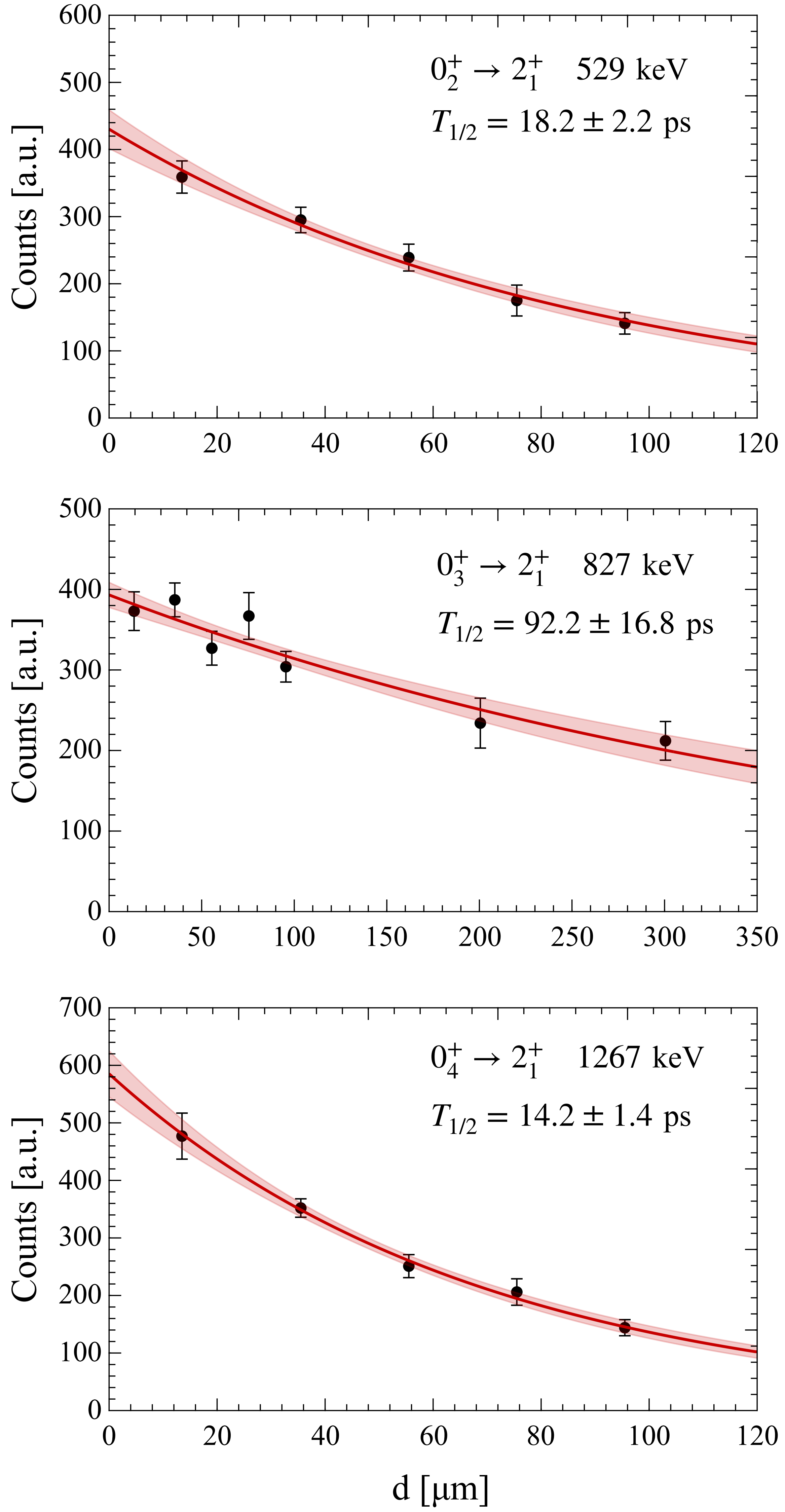

Lifetimes with RDDS

Results from 1n and 2n transfer reactions

- ^{114}Sn ⟹ +2n
- ^{116}Sn ⟹ -1n
- ^{118}Sn ⟹ -1n, +1n
- ^{120}Sn ⟹ -1n

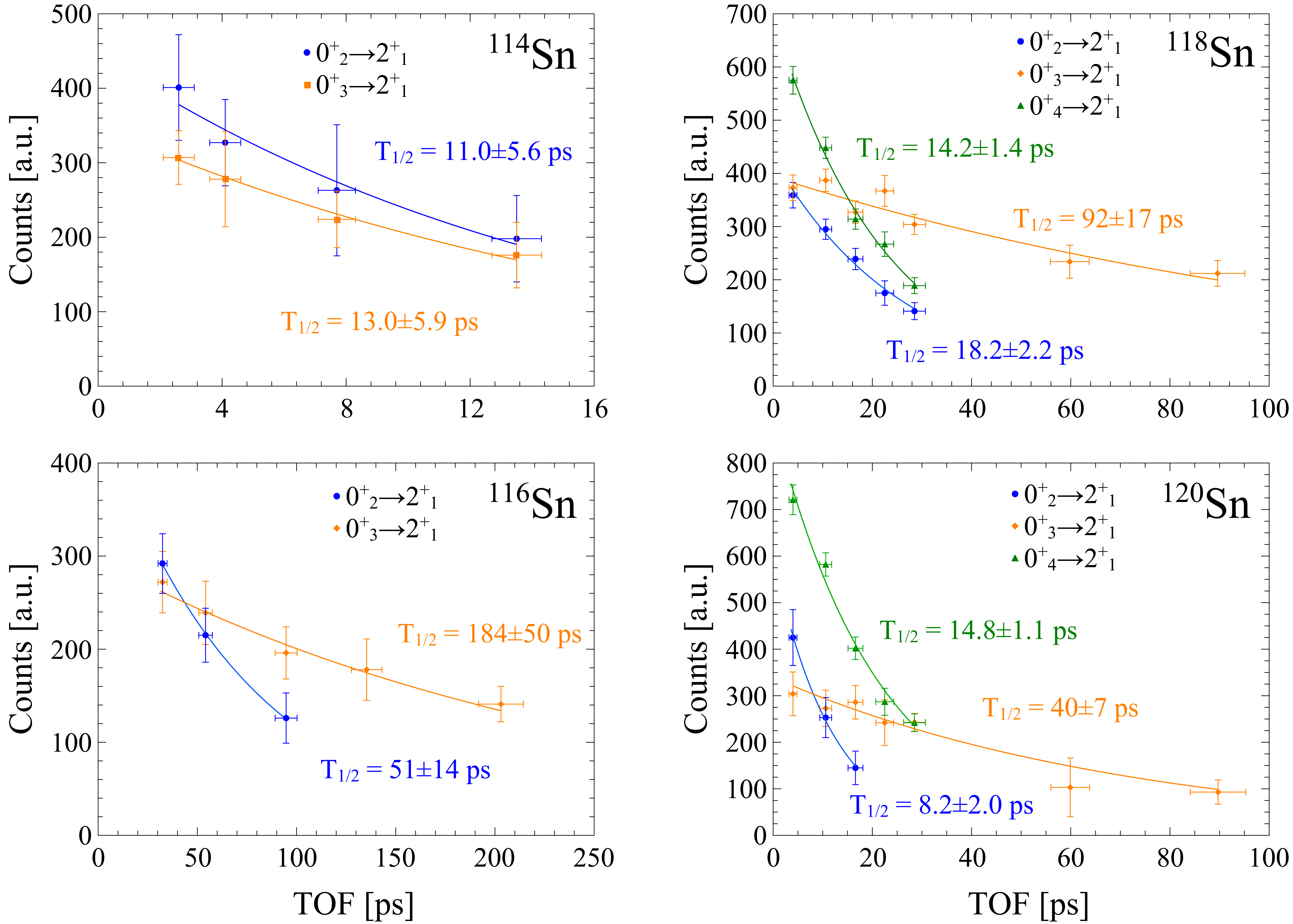

Measured lifetimes of excited 0+ states

Lifetimes of the 0_3^+ in ^{114,118}Sn and all the 0_4^+ measured for the first time!

Good agreement with previously known lifetimes!

This work

Nucleus	E_i [MeV]	I_i^π	$T_{1/2}^{lit}$ [ps]	$T_{1/2}^{exp}$ [ps]
^{114}Sn	1.953	0_2^+	6.5(23)	11.1(56)
	2.156	0_3^+	> 7.6	13.0(59)
	2.422	0_4^+		
^{116}Sn	1.757	0_2^+	44(6), 51(12)[a]	51(14)
	2.027	0_3^+	160(20), 164(10)[a]	184(50)
	2.546	0_4^+		$1.17(^{+0.10}_{-0.09})$
^{118}Sn	1.758	0_2^+	21(3)	18.2(22)
	2.057	0_3^+	< 200	92.2(17)
	2.497	0_4^+		14.2(14)
^{120}Sn	1.875	0_2^+	7.4(10)	8.2(20)
	2.160	0_3^+	34.7(49)[b]	40.4(72)
	2.587	0_4^+	> 0.34	14.8(11)

B(E2) transition probabilities

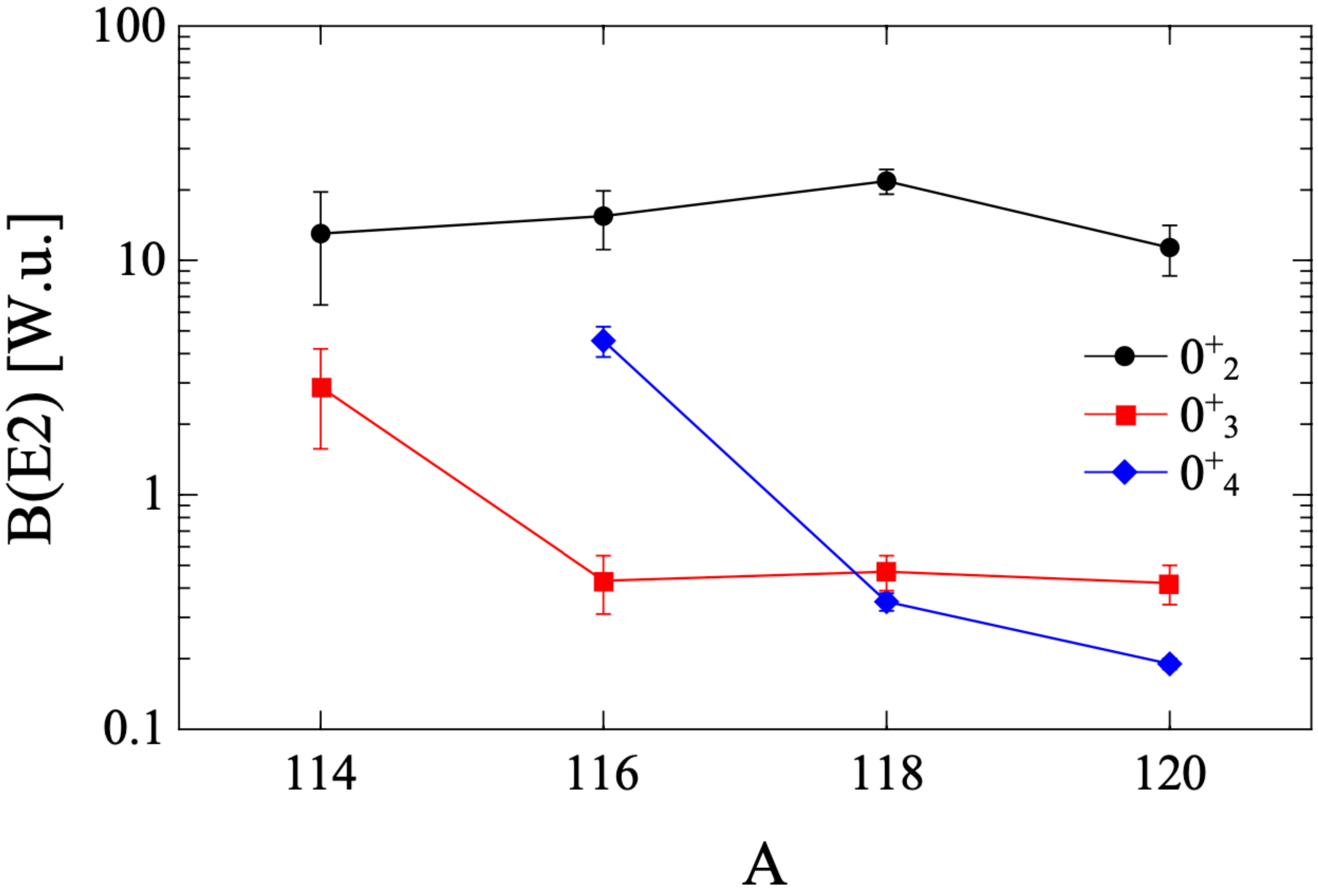

B(E2) systematics hints at structural changes in the microscopic configurations!

Results for ^{114}Sn

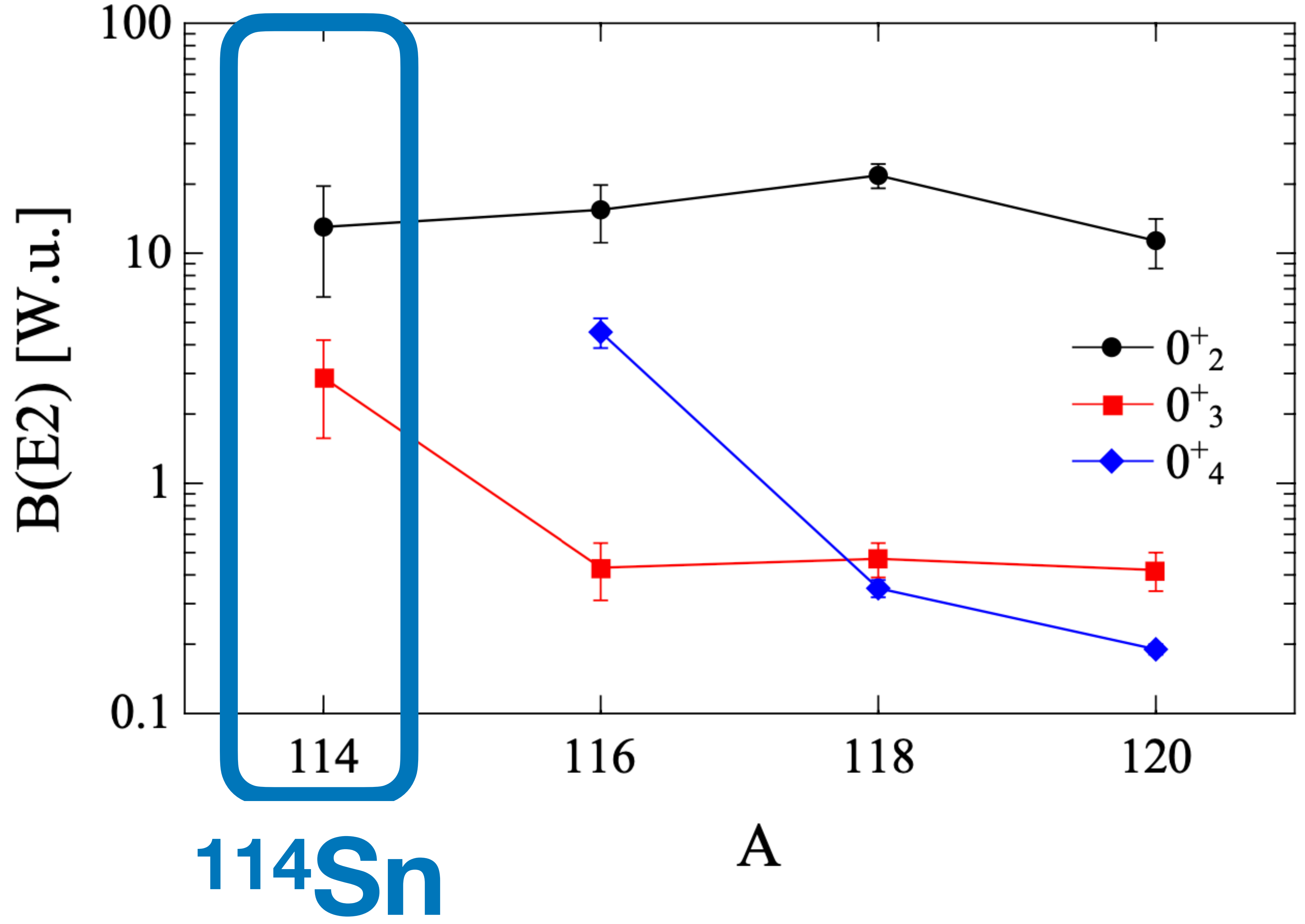

MCSM

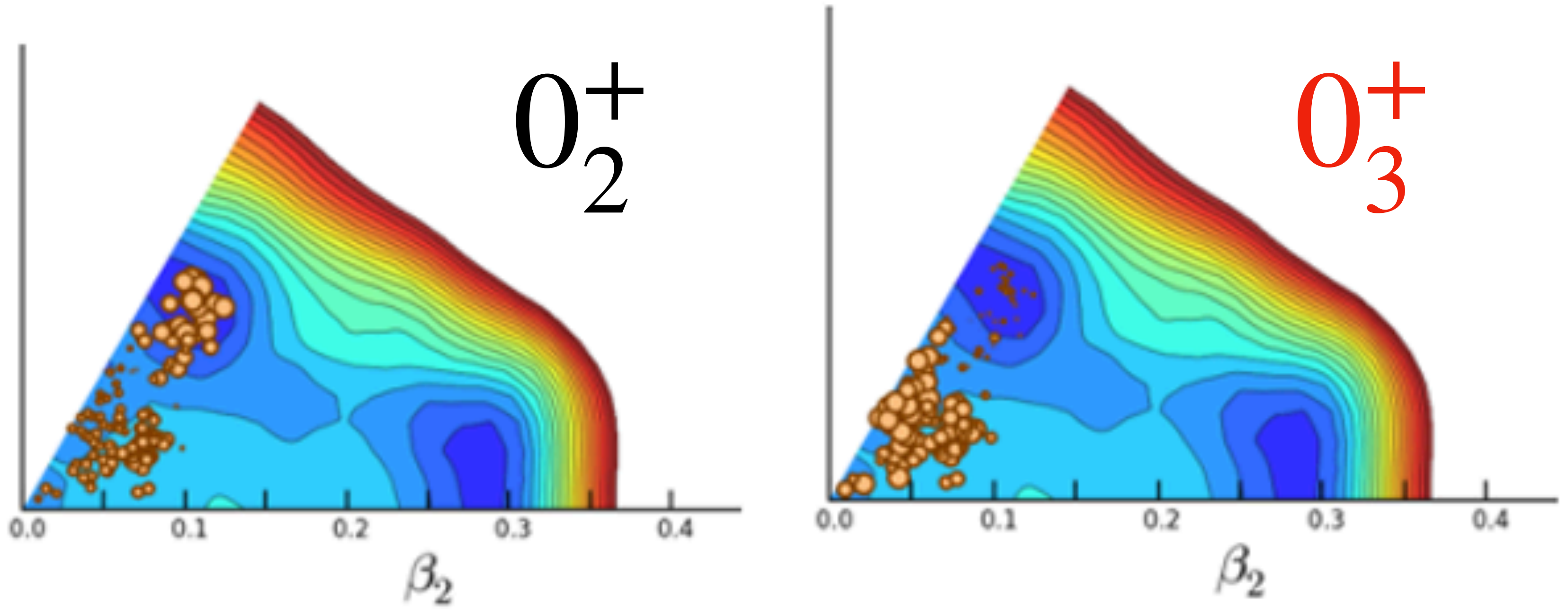

IBM calculations

J_i^π	E_x [MeV]	$E_{x,\mathrm{IBM}}$ [MeV]	J_f^π	$B(E2)_{\mathrm{exp.}}\downarrow$ [W.u.]	$B(E2)_{\mathrm{IBM}}\downarrow$ [W.u.]
Normal configuration					
2_1^+	1.30	1.30	0_1^+	11.1(7)	11
4_1^+	2.19	2.28	2_1^+	5.9(5)	19
0_2^+	1.95	1.99	2_1^+	23.2(8)	21
2_3^+	2.45	2.54	0_1^+	0.023(9)	0.004
Intruder configuration					
0_3^+	2.16	2.15	2_1^+	$\leqslant 5$	2
2_2^+	2.24	2.46	0_1^+	$\leqslant 0.12$	0.04

- Mixing between 0_1^+, 0_2^+ and 0_3^+ based on exp. and theory (MCSM and IBM)
- Both 0_2^+ and 0_3^+ could be band-head of the intruder configuration
- $B(E2; 0_3^+ \rightarrow 2_1^+)$ in good agreement with IBM predictions

M. Spieker et al.,PRC 97, 034319 (2018)

S. Leoni et al., PPNP (2024)

Results for ^{116}Sn

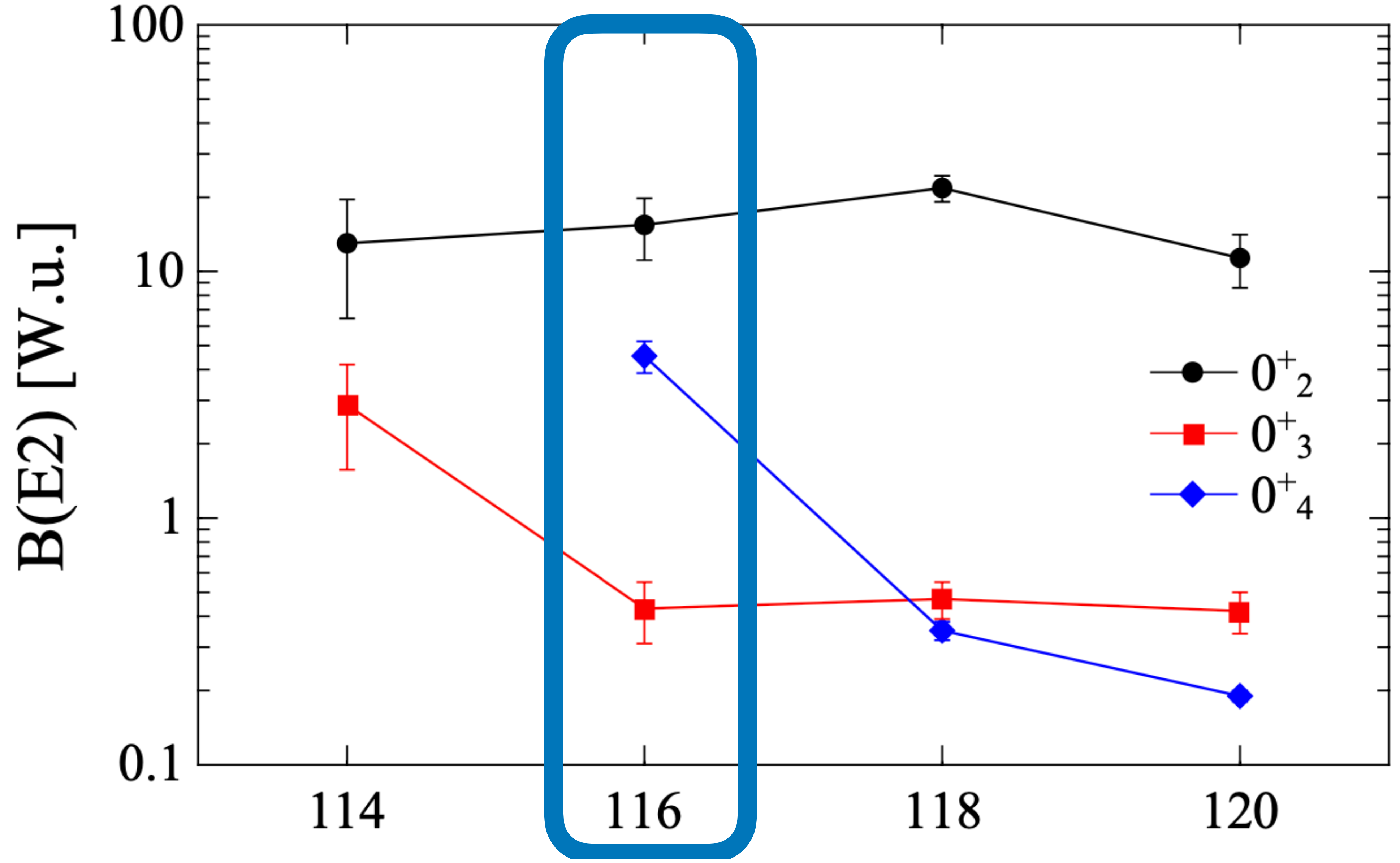

^{116}Sn

MCSM

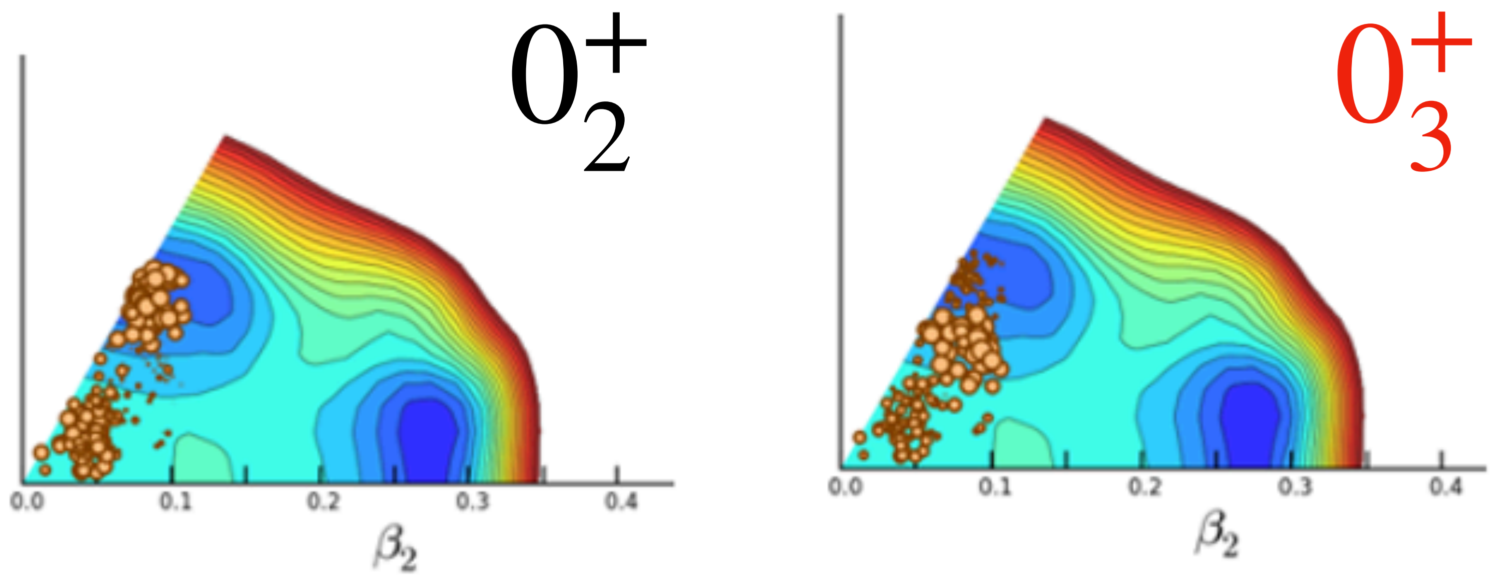

- Consistency with previous measurements, which point to 0_3^+ as band-head of the intruder configuration
- From large $\rho^2(E0)$ between 0_2^+ and 0_3^+, strong mixing and shape difference ($\Delta\beta > 0.23$)
- $B(E2; 0_4^+ \rightarrow 2_1^+) > 1$ W.u. may indicate normal configuration of 0_4^+, in agreement with IBM calculations

C. Petrache et al.,PRC 99 (2019)

S. Leoni et al., PPNP (2024)

Results for ^{118}Sn

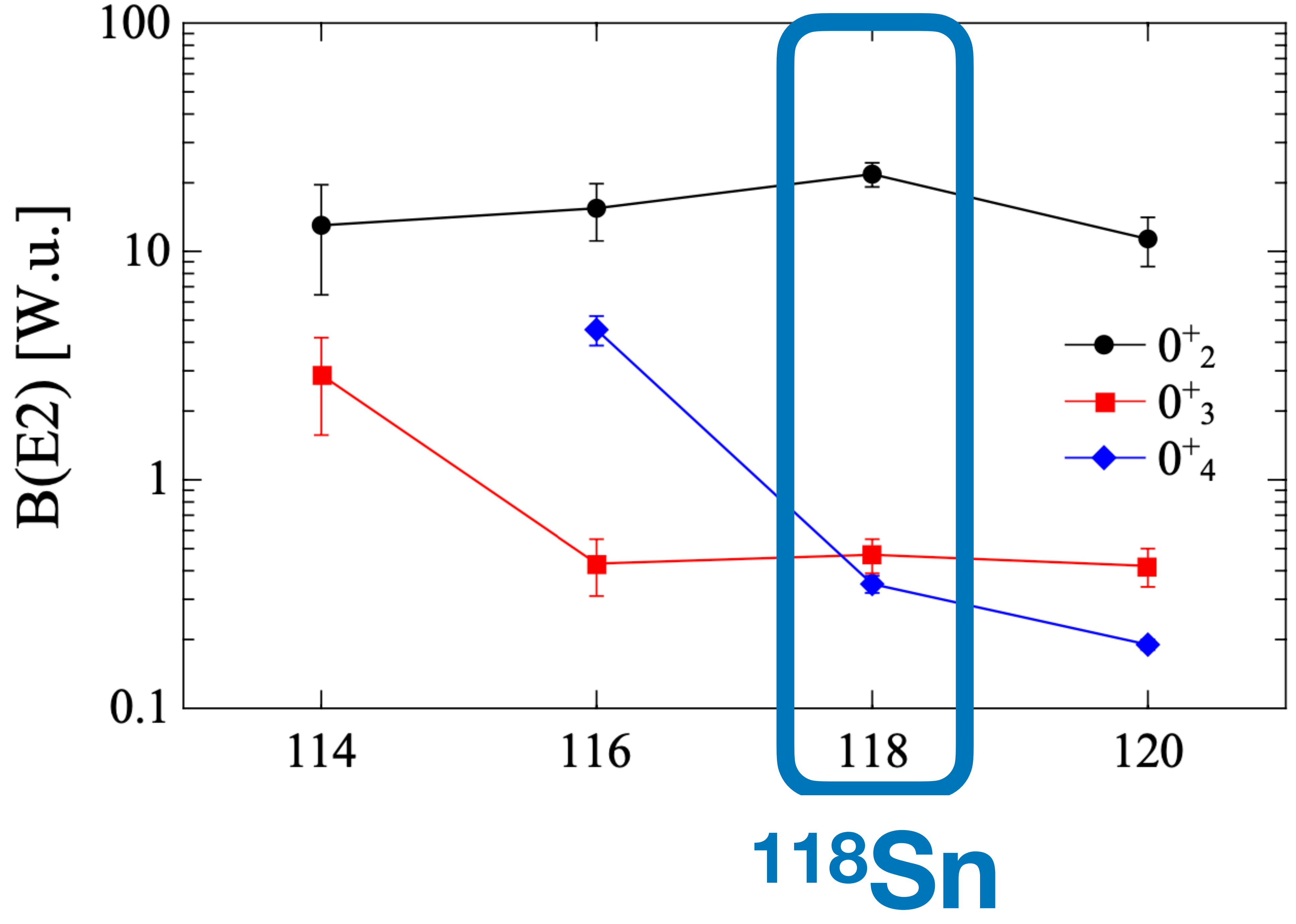

- $B(E2) < 1$ W.u. for 0_3^+ and 0_4^+
- Significant hindrance of the $0_4^+ \rightarrow 2_1^+\ \gamma$
- $\rho^2(E0) = 86(16)$ m.u.

→ Mixing between normal and intruder configurations!

MCSM

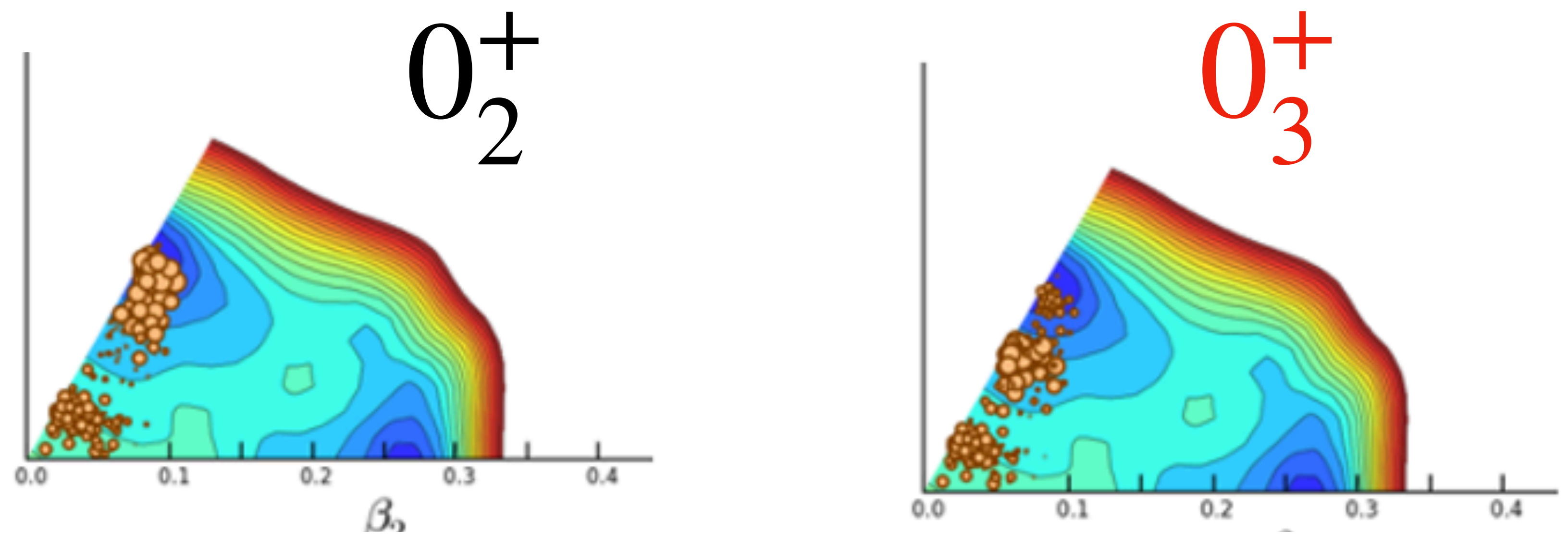

K. Ortner et al., PRC 102 (2020)

K. Ortner et al., PRC 109 (2024)

S. Leoni et al., PPNP (2024)

Results for ^{120}Sn

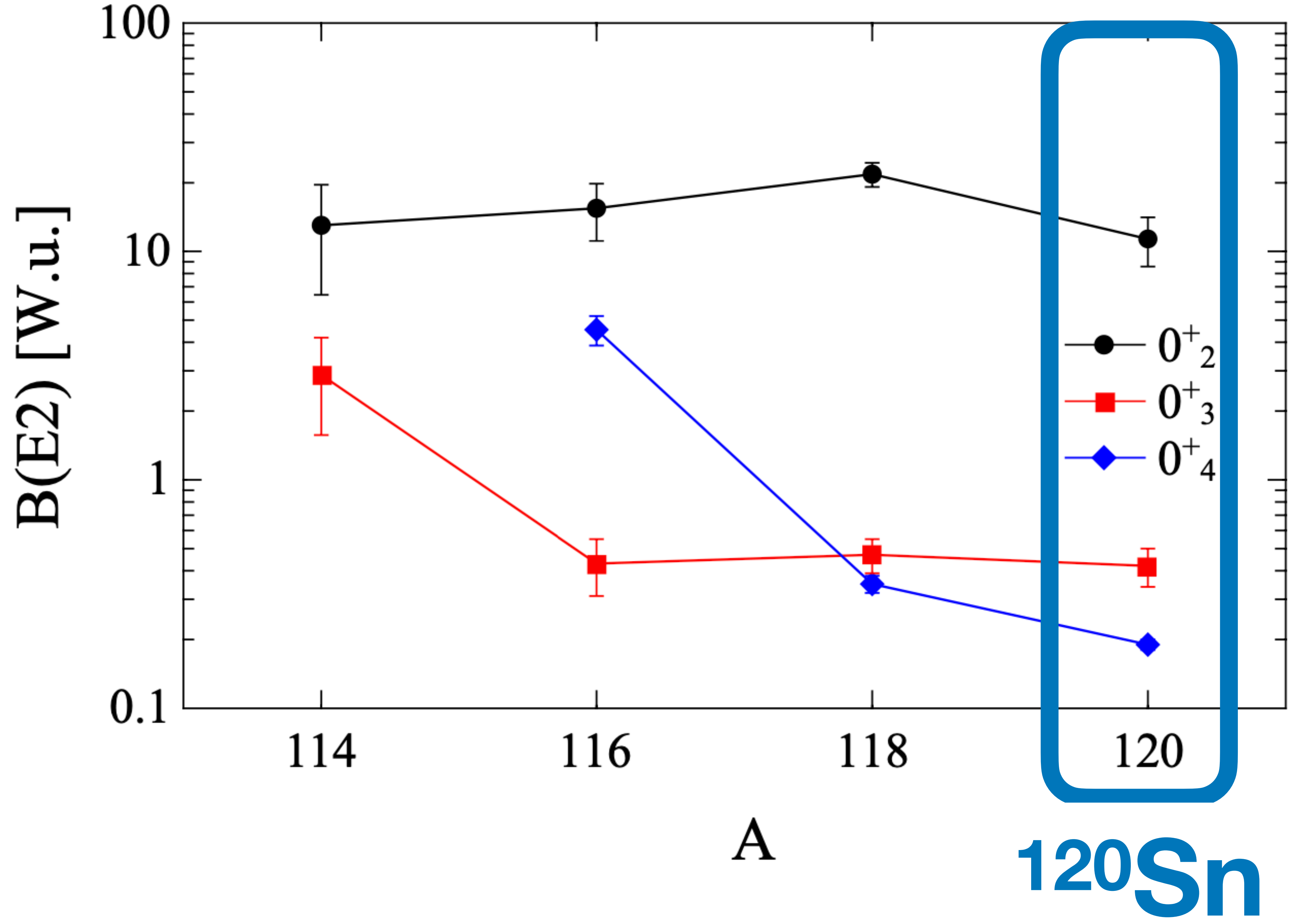

- Analogies with the ^{118}Sn case
- From large $\rho^2(E0)$ between 0^+_2 and 0^+_3, strong mixing and/or shape difference ($\Delta\beta > 0.23$) have been recently estimated
- $B(E2; 0^+_4 \rightarrow 2^+_1)$ = 0.19 W.u.
  Large hindrance factor **HF = 26 !**

MCSM

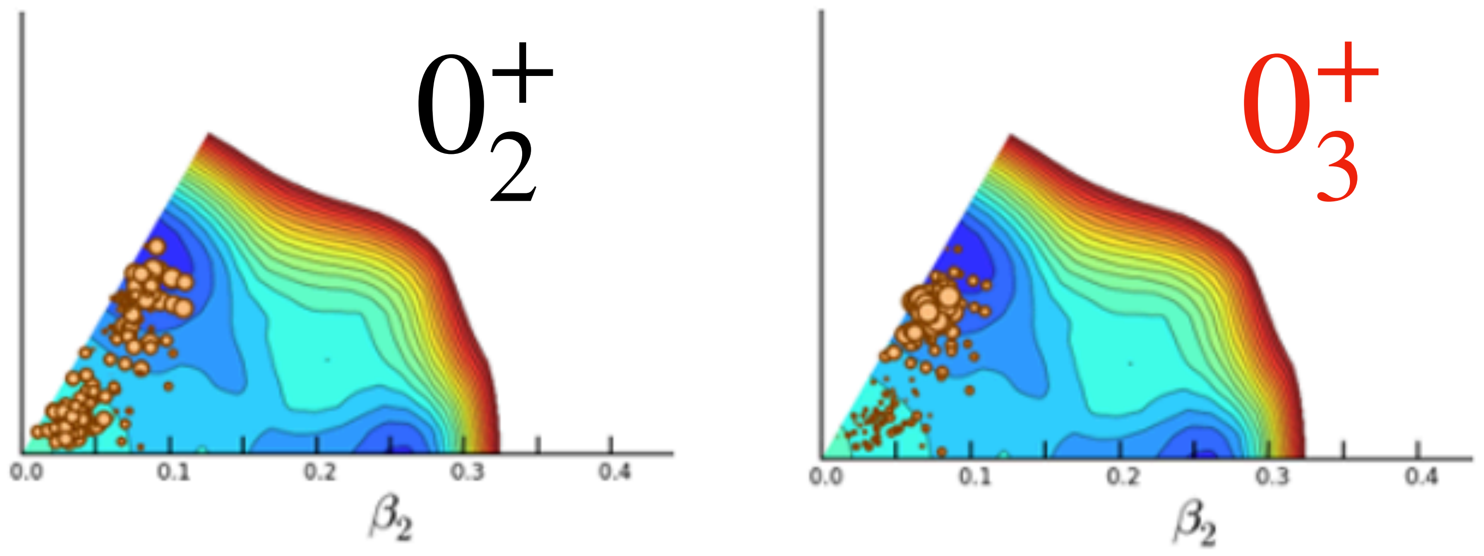

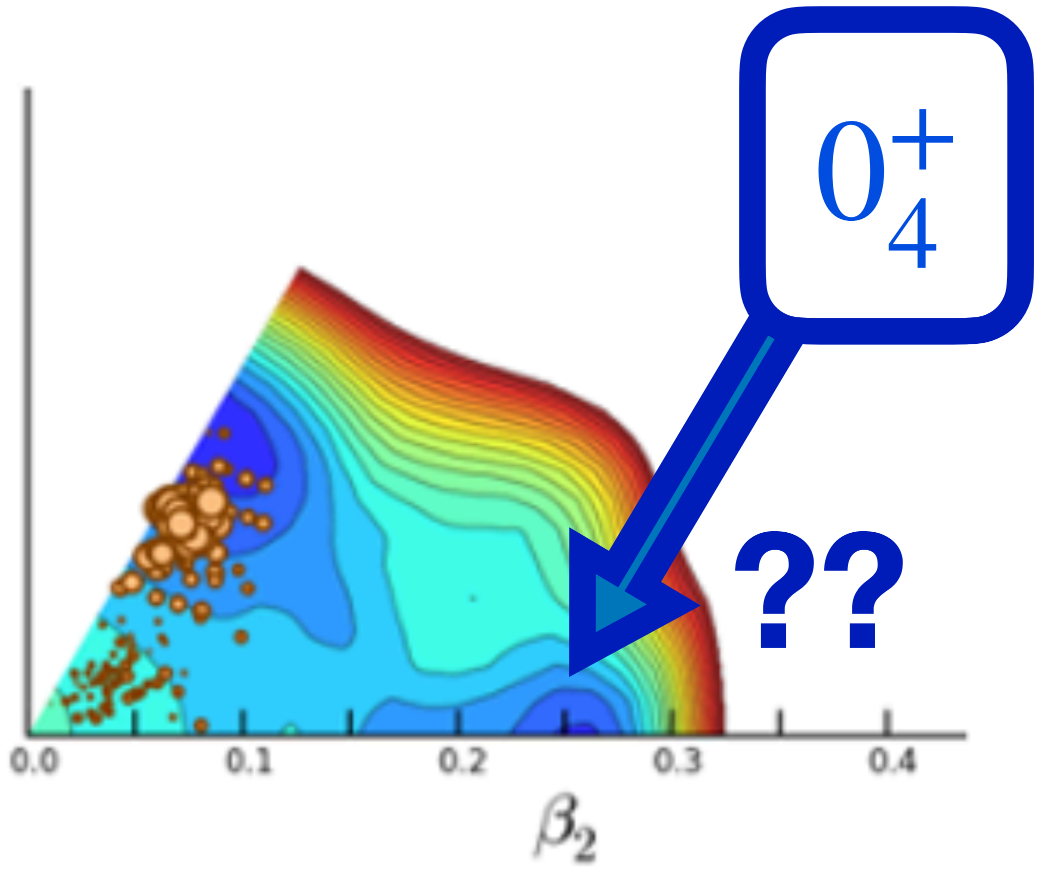

Backlin et al., NPA 351 (1981)
F. Wu et al., PRC 111 (2024)
S. Leoni et al., PPNP (2024)

Summary

- Experimental investigation of shape coexistence in Sn isotopes near the valley of stability
- Heavy-ion transfer reactions at Coulomb barrier energies
- New lifetimes measurements of excited 0^+ states with RDDS and DSAM
- Future comparison with updated theoretical calculations to unveil the complex shape coexistence scenario in the middle of the Z=50 region

Thank you for your attention!

Collaboration:

G. Corbari[1,2], S. Leoni[1,2], B. Fornal[3], N. Mărginean[4], P. Pellegrini[1], S. Bottoni[1,2], F.C.L. Crespi[1,2], M. Ciemała[3], P. Aguilera[7], A.D. Ayangeakaa[11,12], M. Balogh[6], J. Benito[7], G. Benzoni[2], M. Boromiza[4], D. Brugnara[6], F. Camera[1,2], S. Carollo[7], G. Ciconali[1,2], N. Cieplicka-Orynczak[3], C. Clisu-Stan[4], G. Colombi[8,1], C. Costache[4], C. Cuciuc[5], A. Ertoprak[6], R. Escudeiro[7], F. Galtarossa[6], D. Filipescu[4], N. Florea[4], I. Gheorge[4], A. Goasduff[6], A. Gottardo[6], A. Ionescu[4], Ł. Iskra[3], R.V.F. Janssens[11,12], S.M. Lenzi[7], R. Lică[4], R. Mărginean[4], M. Matejska-Minda[3], D. Mengoni[7], C. Michelagnoli[8], C. Mihai[4], B. Million[2], D.R. Napoli[6], C. Neacșu[4], A. Negreț[4], C.R. Niță[4], A. Olăcel-Coman[4], T. Otsuka[10], J. Pellumaj[6], R.M. Pèrez-Vidal[6], S. Pigliapoco[7], E. Pilotto[7], M. Polettini[7], F. Recchia[7], K. Rezynkina[7], M. Sedlak[6], M. Sferrazza[9], L. Stan[4], Y. Tsunoda[10], A. Turturică[4], S. Ujeniuc[4], J.J. Valiente-Dobòn[6], O. Wieland[2], I. Zanon[6], L. Zago[7], G. Zhang[7], H. Zhen[7]

[1] Dipartimento di Fisica, Università degli Studi di Milano, Italy
[2] INFN, Sezione di Milano, Italy
[3] Institute of Nuclear Physics, IFJ-PAN, Krakow, Poland
[4] Horia Hulubei National Institute for Physics and Nuclear Engineering, Măgurele, Romania
[5] Extreme Light Infrastructure, Nuclear Physics, Măgurele, Romania
[6] INFN, Laboratori Nazionali di Legnaro, Italy
[7] Dipartimento di Fisica and INFN, Sezione di Padova, Padova, Italy
[8] Institut Laue-Langevin, Grenoble, France
[9] Université libre de Bruxelles (ULB), Belgium
[10] University of Tokyo, Tokyo, Japan
[11] University of North Carolina at Chapel Hill, USA
[12] Triangle Universities Nuclear Laboratory, Duke University, USA

Shell evolution: type II

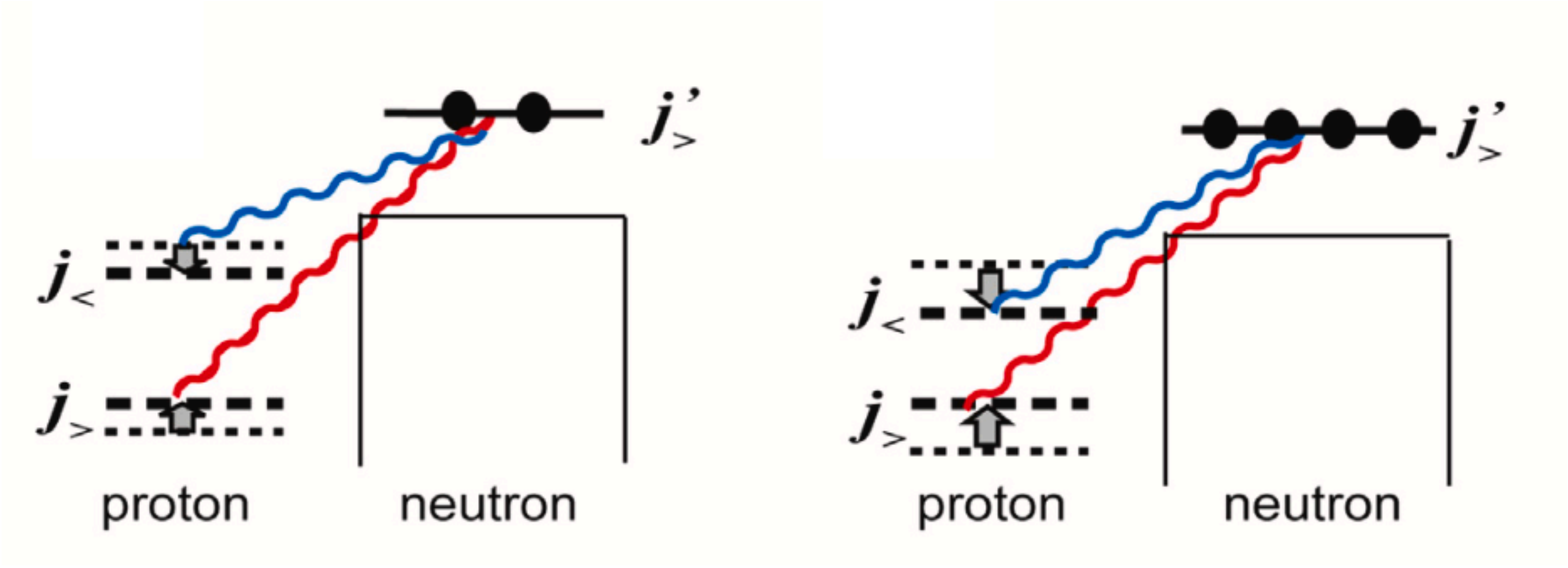

The **monopole** part of the tensor force **reduces** the proton spin-orbit splitting

T. Otsuka, et al., Rev. Mod. Phys. 92 (2020) 015002

S. Leoni et al., Phys. Rev. Lett. 118, 162502 (2017)

N. Mărginean et al., Phys. Rev. Lett. 125, 102502 (2020)

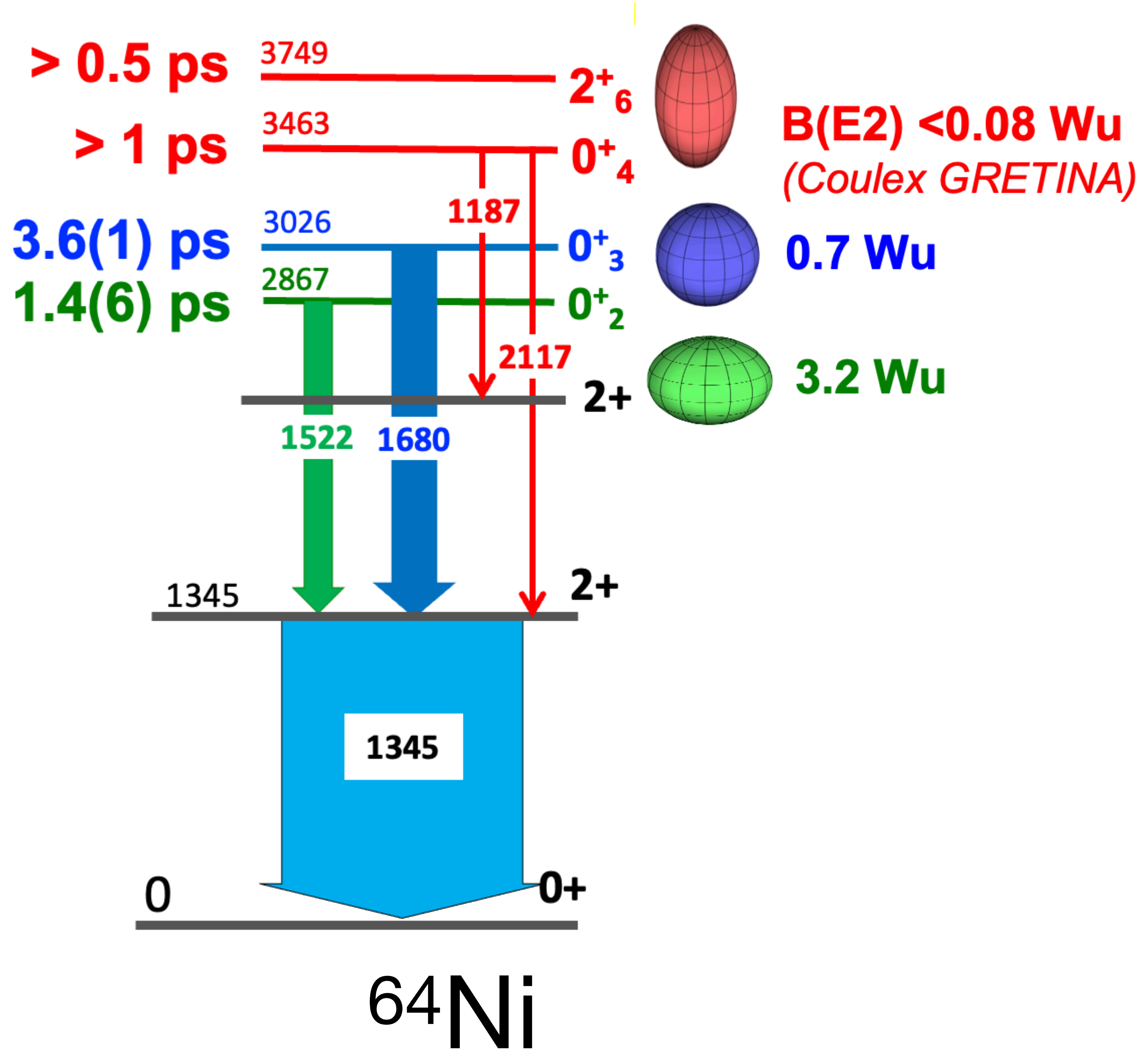

Coexistence of **spherical, oblate and prolate 0+** excitations in ^{64}Ni and ^{66}Ni

ROSPHERE simulations

Inputs parameters and files

- Target+backing thicknesses
- Reaction profiles
  - *Normalized cross section as a function of the depth in the target*
- Angular distributions
  - *Calculated with the GRAZING code*
- Energy loss tables
  - *Geant4 energy loss calculations*
- Response function of the HPGe
  - *Measured FWHM curved*

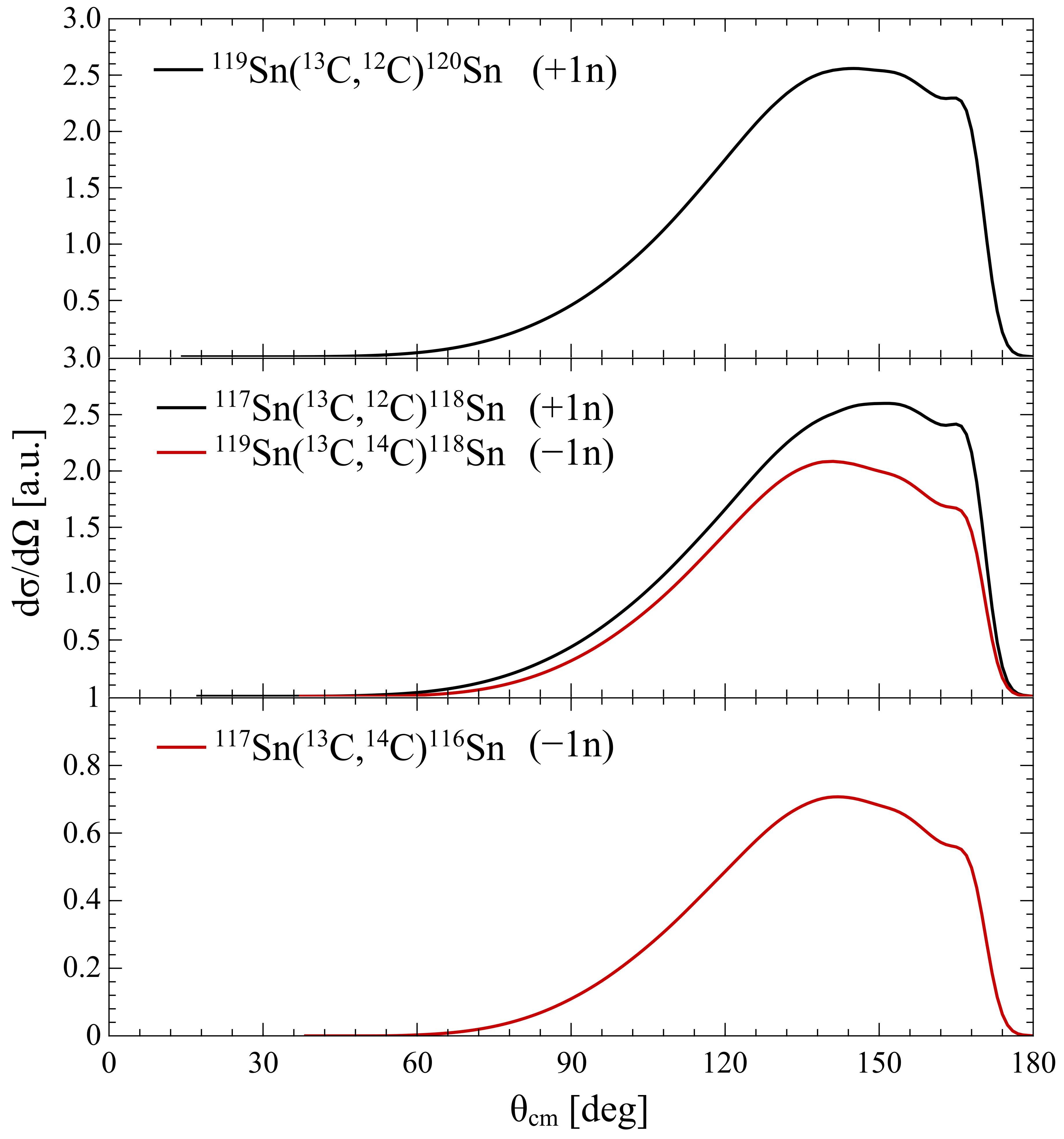

ROSPHERE simulations

Inputs parameters and files

- Target+backing thicknesses
- Reaction profiles
  - *Normalized cross section as a function of the depth in the target*
- Angular distributions
  - *Calculated with the GRAZING code*
- Energy loss tables
  - *Geant4 energy loss calculations*
- Response function of the HPGe
  - *Measured FWHM curved*

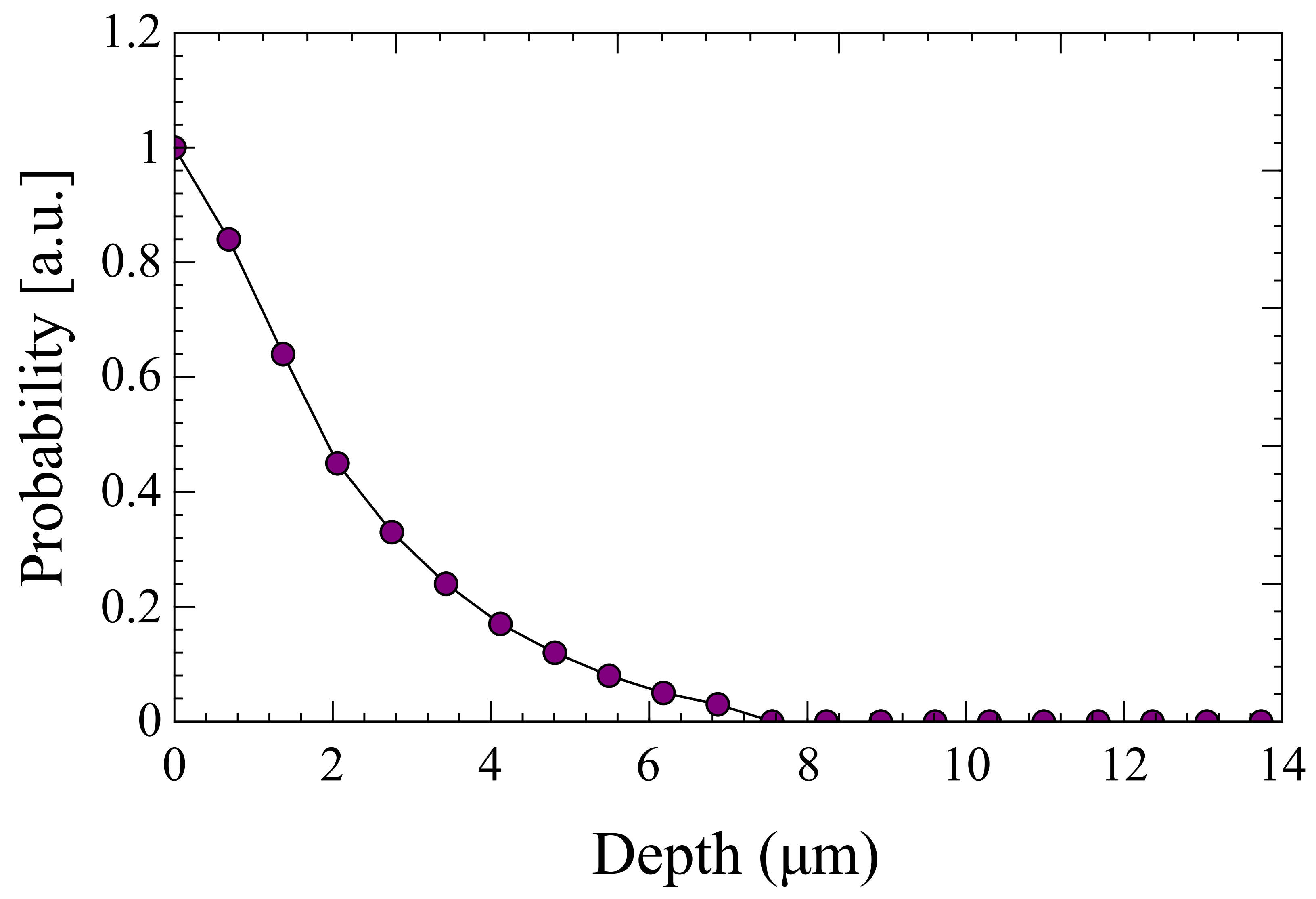

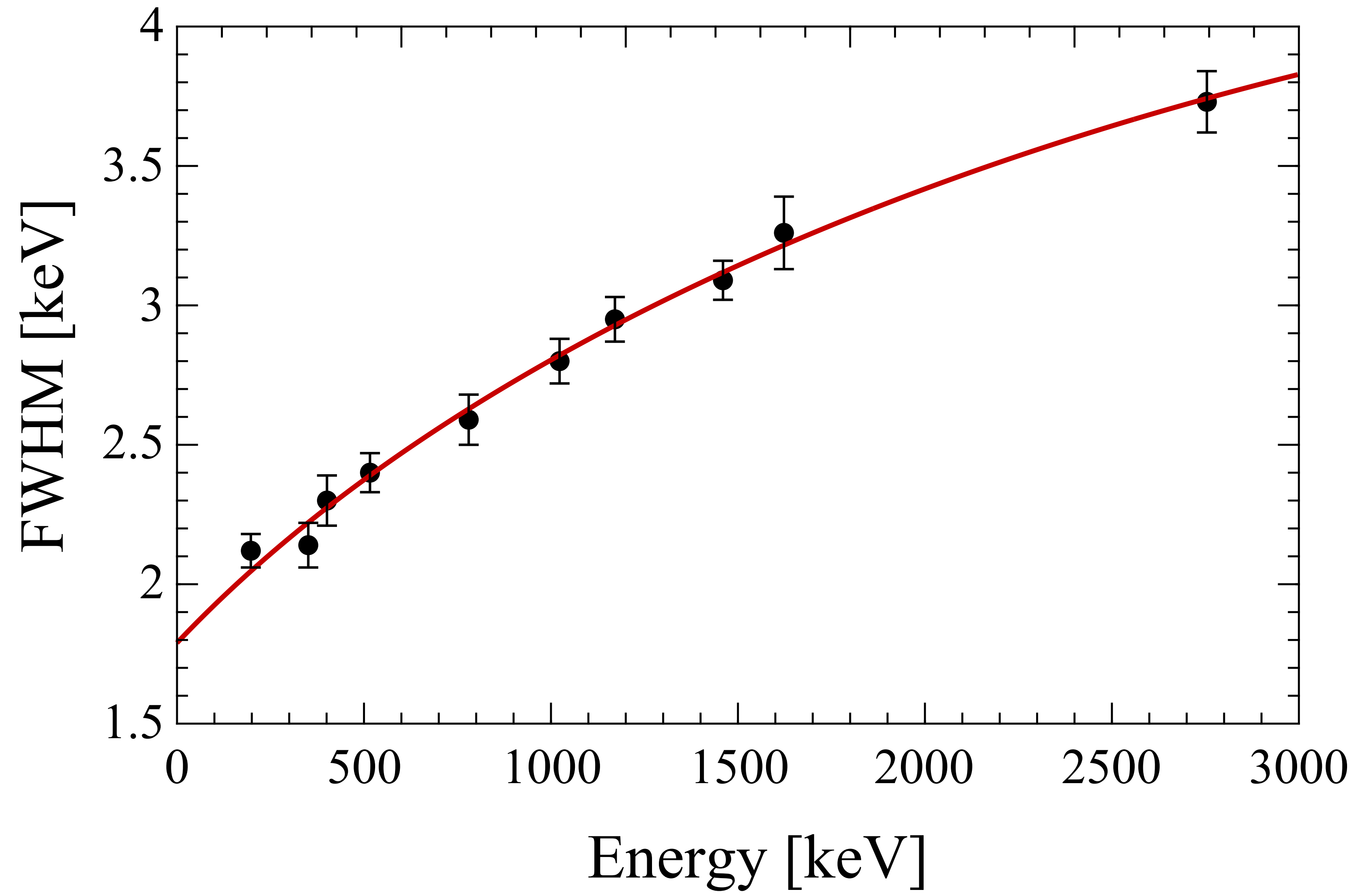

Velocity estimation

Plunger measurements performed without particle coincidences

Non-Gaussian shape of the shifted component prevents simple beta estimation

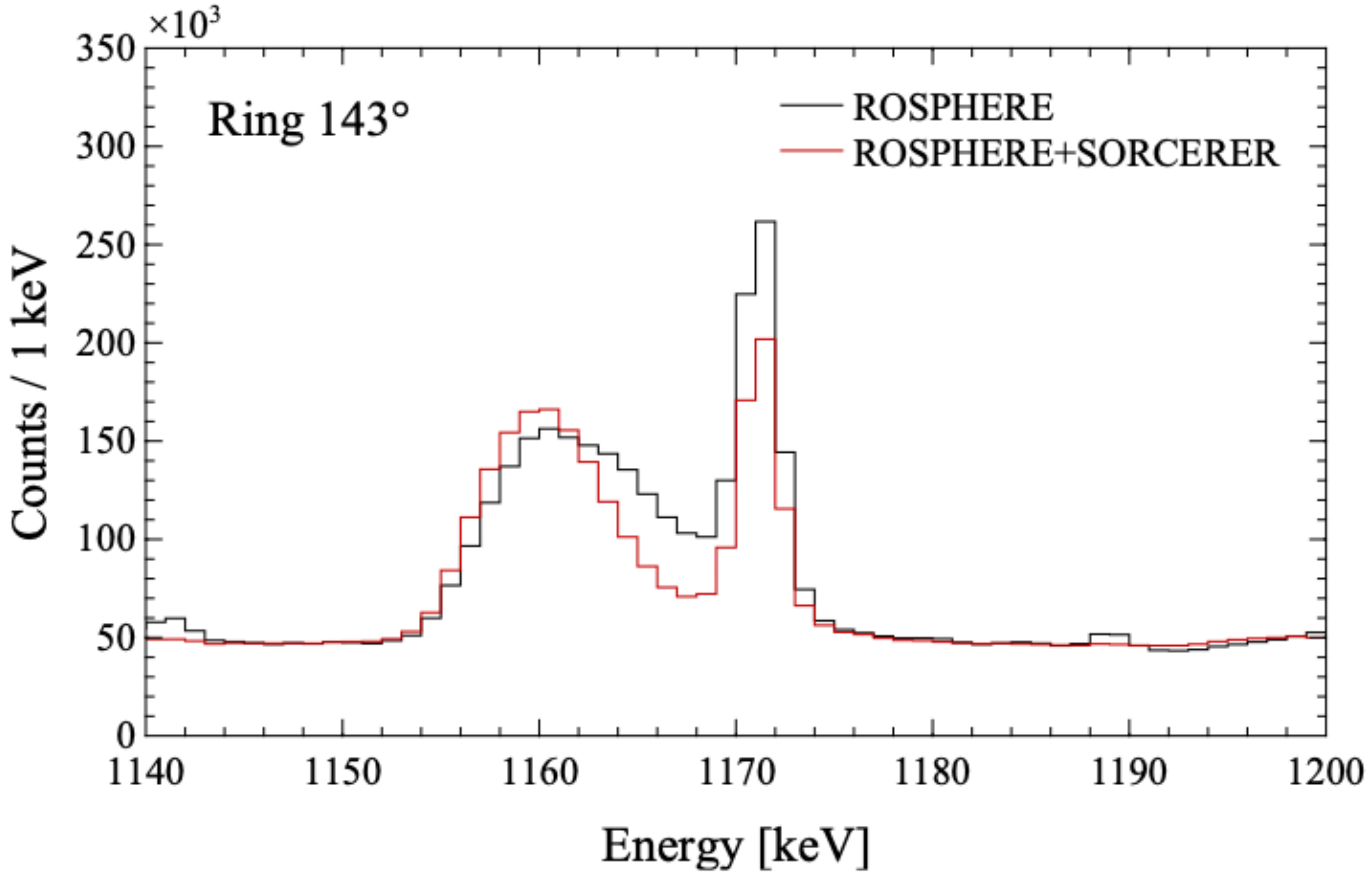

Doppler-correction Optimization

Optimum <β>

based on the best doppler correction coefficients

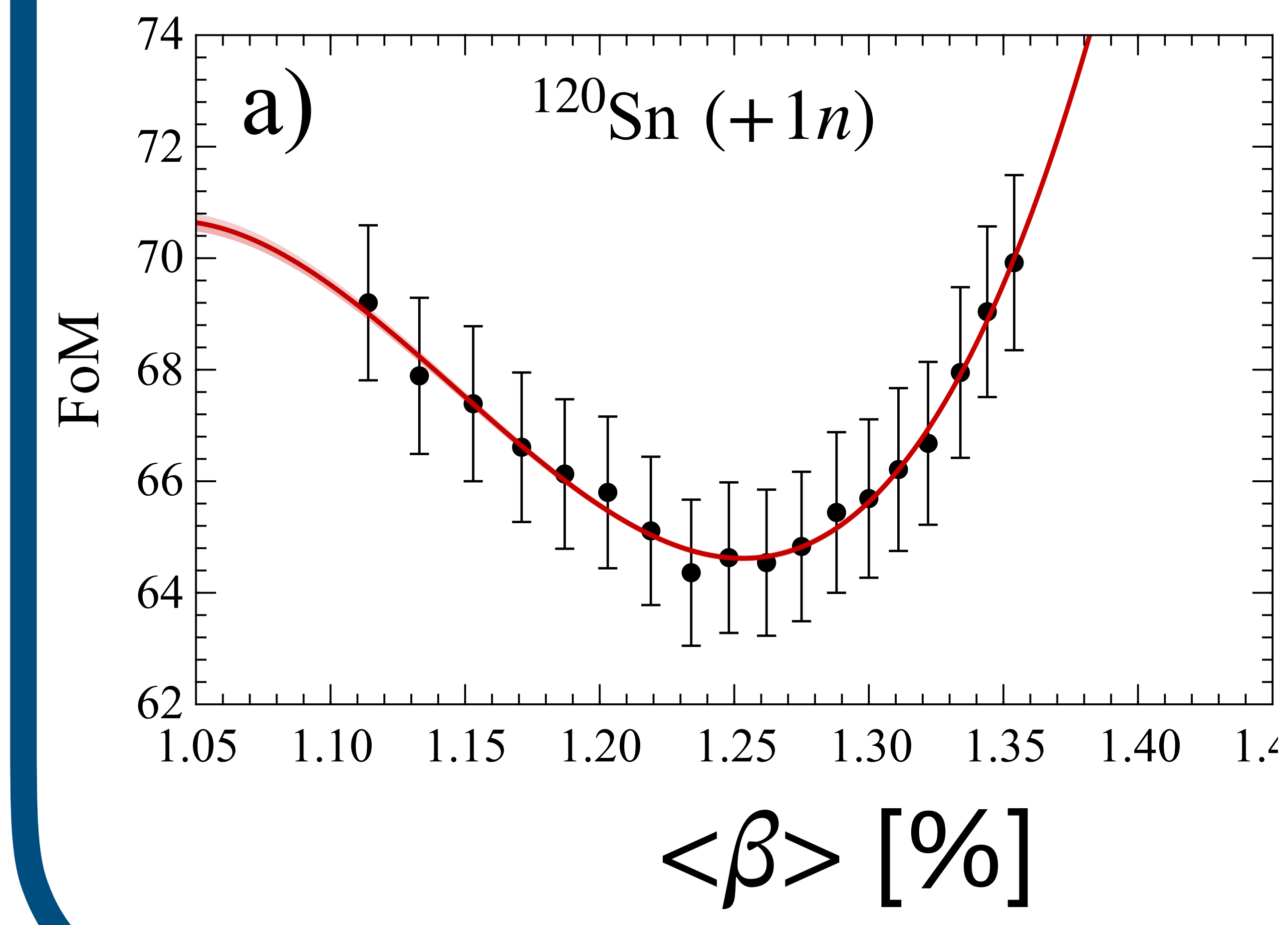

Bootstrapping method

Uncertainty on <β>

from Monte Carlo resampling of the data points

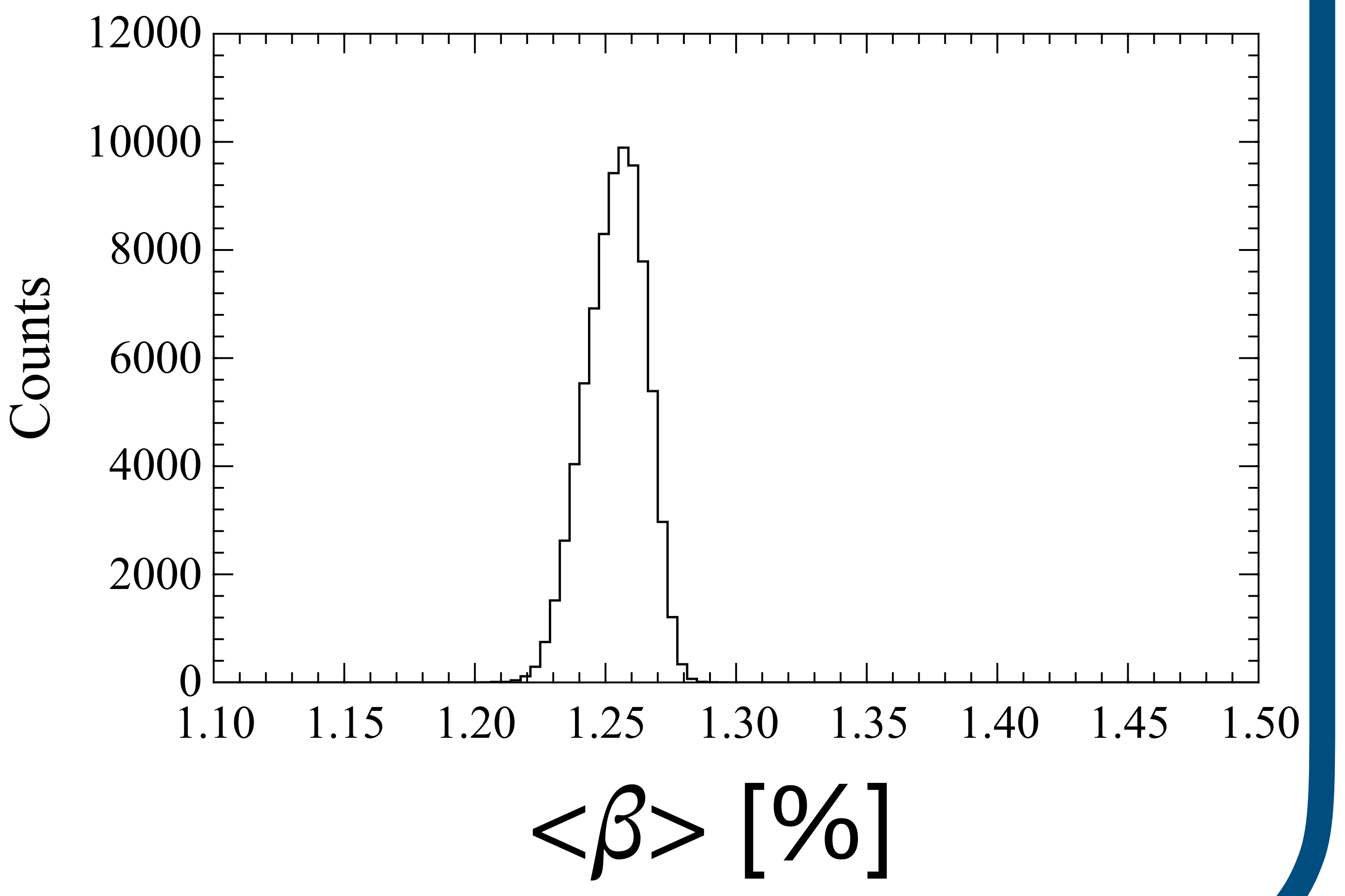

Backup: Recent Ni measurements

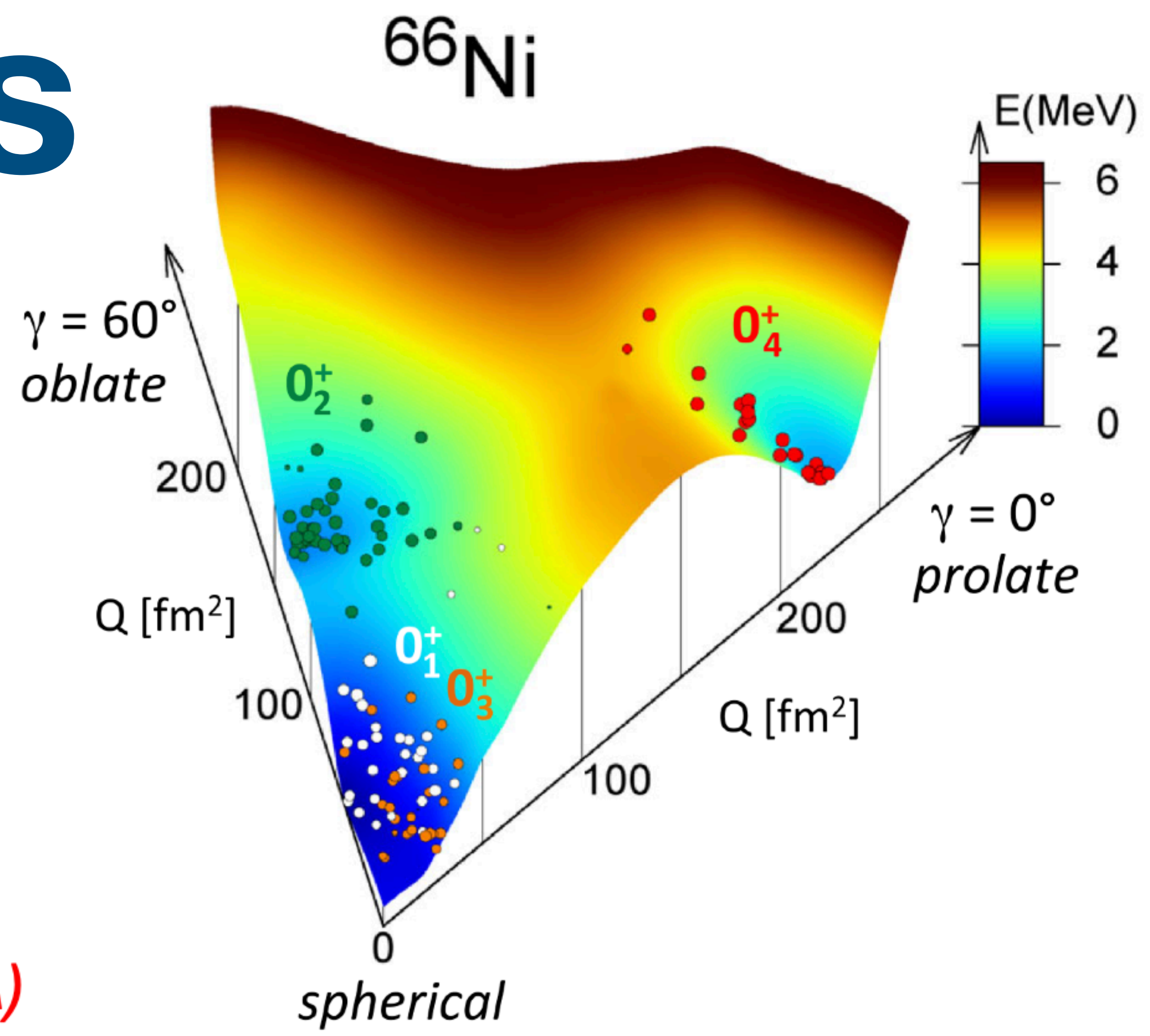

Coexistence of **spherical, oblate and prolate 0+** excitations in ^{64}Ni and ^{66}Ni

Shape isomer-like:

- B(E2) < 0.08 in ^{64}Ni
- B(E2) = 0.2 in ^{66}Ni

prolate → spherical transition

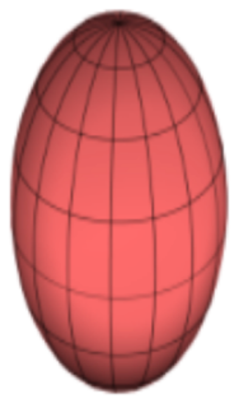

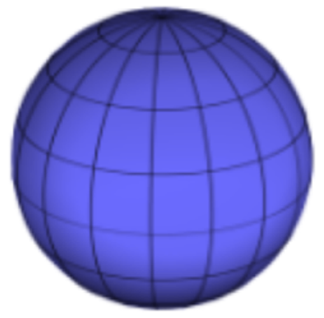

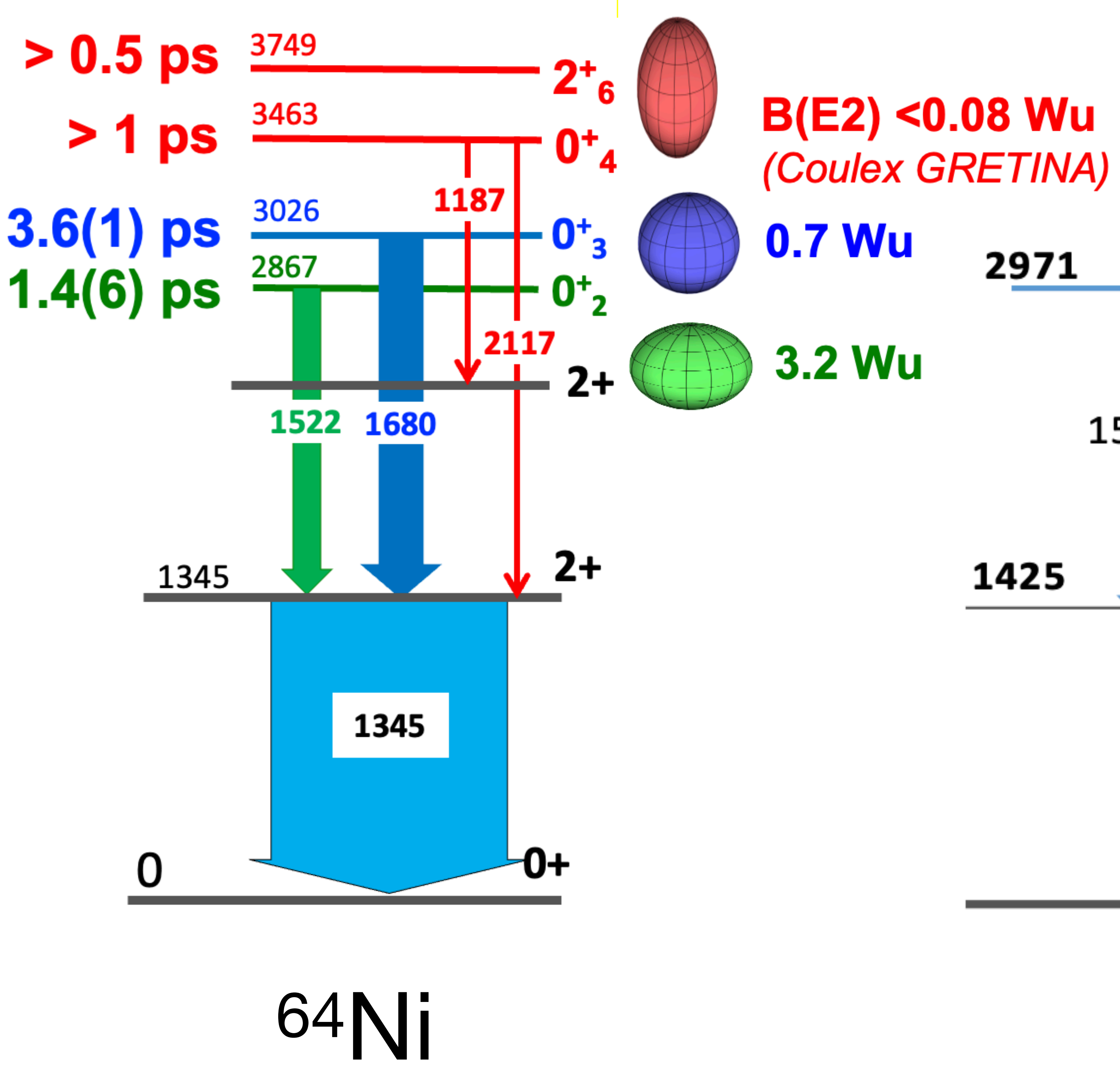

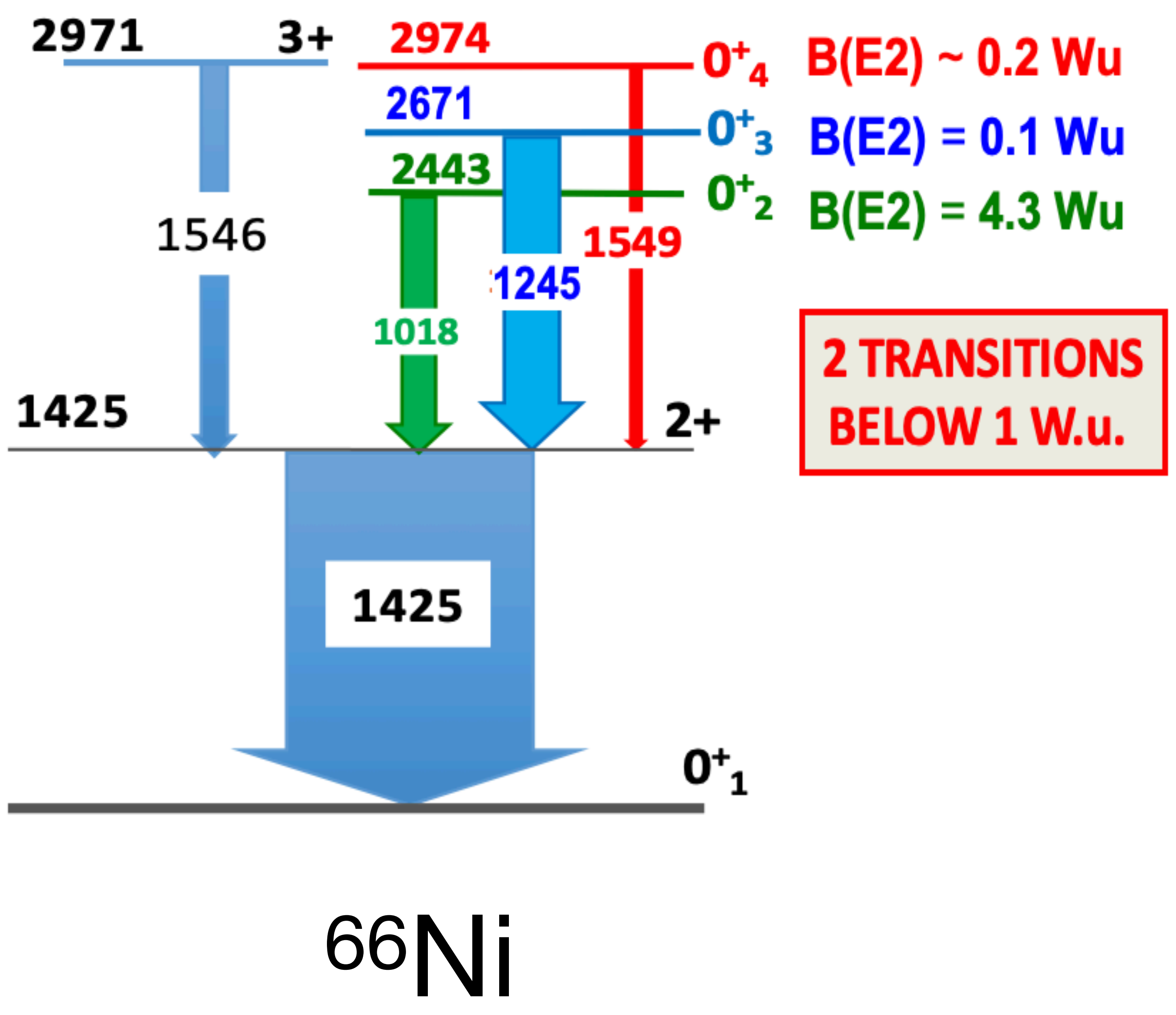

S. Leoni et al., Phys. Rev. Lett. 118, 162502 (2017)

N. Mărginean et al., Phys. Rev. Lett. 125, 102502 (2020)

Backup - Monopole-driven excitations

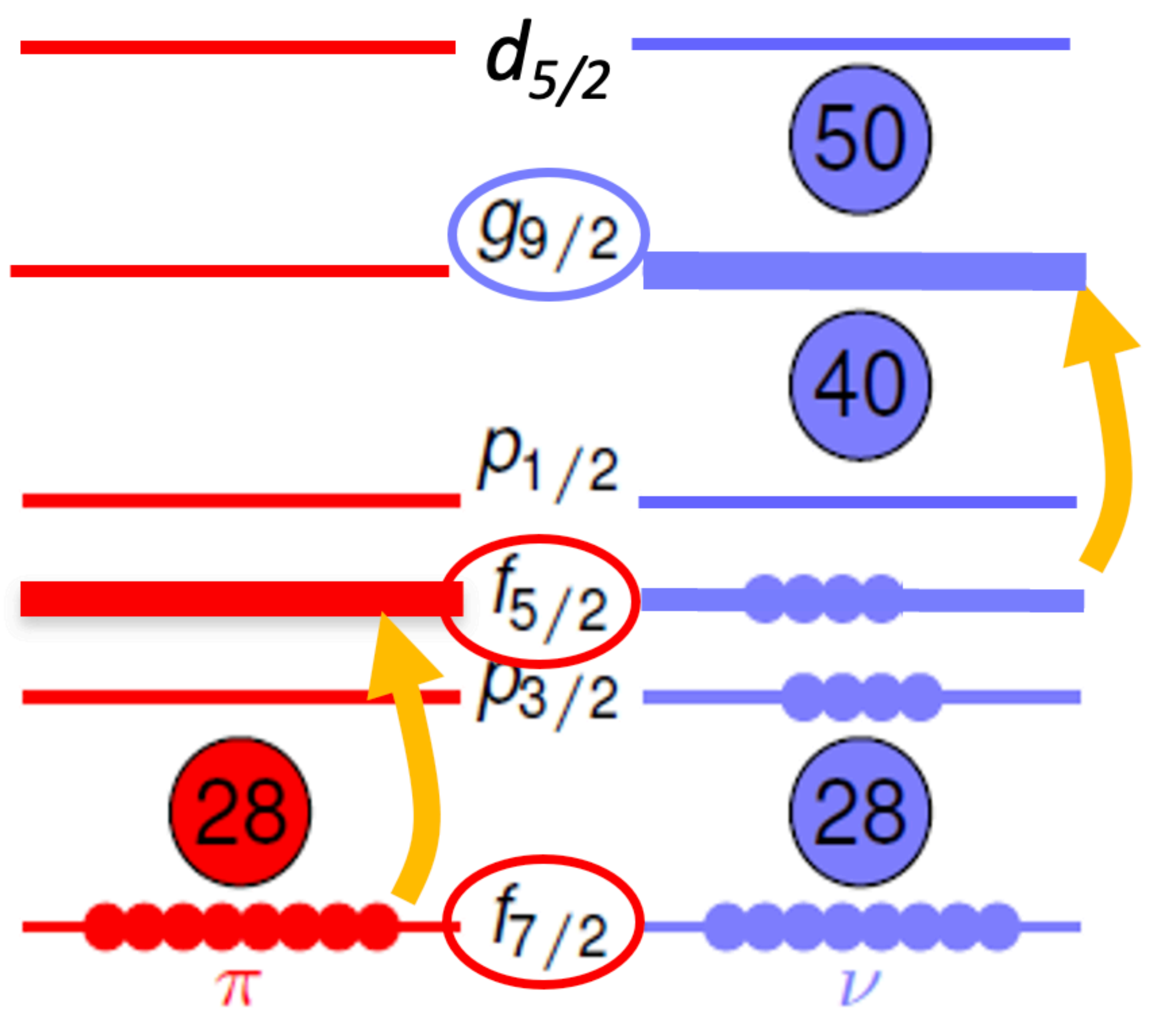

^{64}Ni

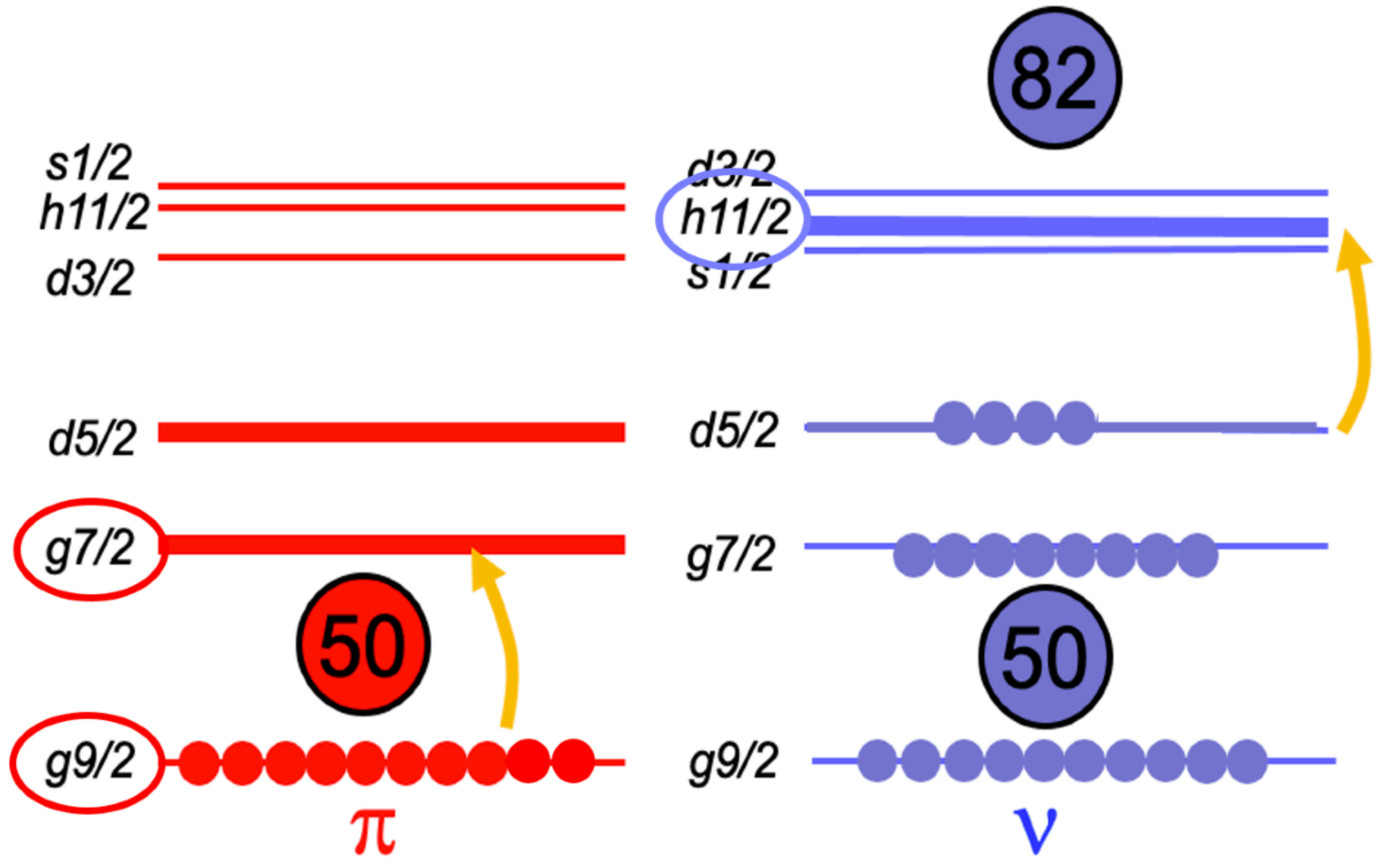

^{112}Sn

- Spontaneus symmetry breaking due to p-n interaction
- Driven by the **monopole part of the tensor force**
- Neutron excitation in $g_{9/2}$ induces a **reduction** of the **$f_{5/2}$-$f_{7/2}$ splitting** (Z=28 shell gap)

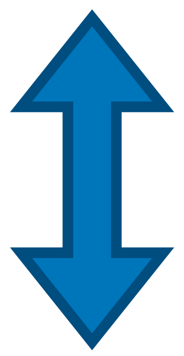

Analogy with $^{112\text{-}114}$Sn isotopes

Neutron excitation in $h_{11/2}$ induces a **reduction** of the **$g_{7/2}$-$g_{9/2}$ splitting** (Z=50 shell gap)

S. Leoni et al., Phys. Rev. Lett. 118, 162502 (2017)

N. Mărginean et al., Phys. Rev. Lett. 125, 102502 (2020)

Backup - MCSM calculations

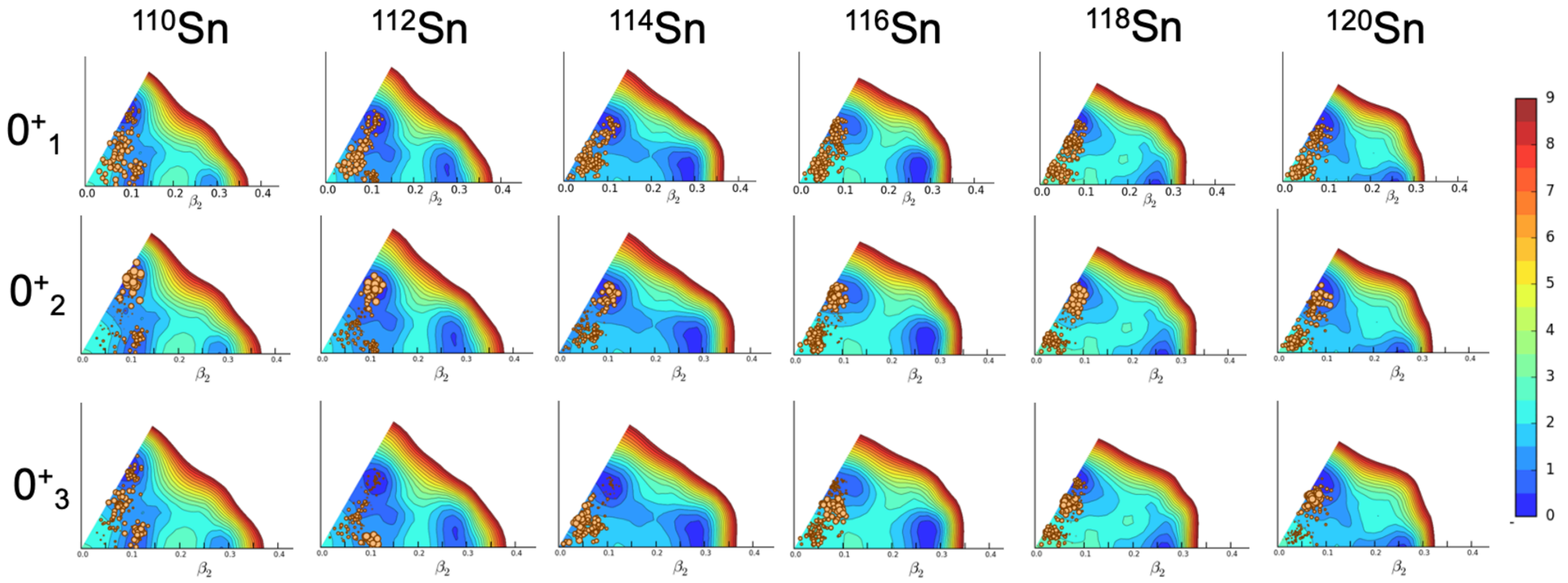

Preliminary calculations!

T. Otsuka, Y. Tsunoda, to be published.

T. Togashi et al., Phys. Rev. Lett. 121, 062501 (2018).

Lifetime results

Lifetimes of the 0_3^+ in ^{114,118}Sn and all the 0_4^+ measured for the first time!

Good agreement with previously known lifetimes!

Nucleus	E_i [MeV]	I_i^π	$T_{1/2}^{lit}$ [ps]	$T_{1/2}^{exp}$ [ps]
^{114}Sn	1.953	0_2^+	6.5(23)	11.1(56)
	2.156	0_3^+	> 7.6	13.0(59)
	2.422	0_4^+		
^{116}Sn	1.757	0_2^+	44(6), 51(12)[a]	51(14)
	2.027	0_3^+	160(20), 164(10)[a]	184(50)
	2.546	0_4^+		$1.17(^{+0.10}_{-0.09})$
^{118}Sn	1.758	0_2^+	21(3)	18.2(22)
	2.057	0_3^+	< 200	92.2(17)
	2.497	0_4^+		14.2(14)
^{120}Sn	1.875	0_2^+	7.4(10)	8.2(20)
	2.160	0_3^+	34.7(49)[b]	40.4(72)
	2.587	0_4^+	> 0.34	14.8(11)

Evolution of single particle states